Title
Constitutive Syk Activity Deregulates Cell Signaling and Hematopoiesis

Author
Graham, Michelle T.

Publication Date
2012

Peer reviewed|Thesis/dissertation

Constitutive Syk Activity Deregulates Cell Signaling and Hematopoiesis

by

Michelle Toft Graham

DISSERTATION

Submitted in partial satisfaction of the requirements for the degree of

DOCTOR OF PHILOSOPHY

in

Biomedical Sciences

in the

GRADUATE DIVISION

of the

UNIVERSITY OF CALIFORNIA, SAN FRANCISCO

ACKNOWLEDGEMENTS

I would like to thank my mentor, Dr. Clifford Lowell for his guidance, patience, and support. Cliff fosters a convivial laboratory atmosphere and always welcomes questions, concerns, and comments regardless of failures and successes. I had many failures and I appreciate that Cliff took the time confront them with me.

I would like to thank my committee members, Dr. Neil Shah, Dr. Michelle Hermiston, and Dr. Kevin Shannon for their insightful comments and questions. Thesis committee meetings were often uplifting and inspirational and I thank you for providing motivation to tackle many of my projects obstacles. I would also like to thank my graduate advisor Dr. Anita Sil for her understanding and support, especially during the early years of my thesis work, as well as providing guidance for work beyond graduate school and into my postdoctoral work.

Thanks also to the Biomedical Sciences program for providing me with the opportunity to pursue my dreams in the health-related science field. Without their tireless assistance and cheerful encouragement, the graduate school process would have been even more bewildering and overwhelming.

I would like to thank my patient laboratory mates, present and past, for their relentless support and encouragement. I would especially like to thank Yongmei Hu and Dr. Clare Abram for their cooperation on both the TEL-Syk and allelic series portion of my dissertation. Both provided unparalleled expertise and support that was vital to the success of these projects. Drs. Lynn Kamen, Allison Miller, Patrizia Scapini and Jessica Van Ziffle imparted bountiful advice that was instrumental in the foundation of the

projects and I greatly appreciate their cooperative spirit. Finally I would like to thank Dr. Emily Elliott for her support as a fellow graduate student and friend. Without Emily life in the laboratory and graduate school would have been drab and monotonous.

I would like to thank Dr. Hassan Jumaa for providing the TEL-Syk fusion, Jennifer Bolen and Loretta Chan for histology and cleaved caspase-3 IHC assistance, Tara Rambaldo for help with flow cytometry and cell sorting. I would also like to thank Dr. Arthur Weiss for his comments and suggestions for the allelic series project.

Graduate school could not have been tolerable without the support and camaraderie of Allison Coady, Rebecca Lock, Tobias Gerdes, Morgan Truitt, and Lilliana Radoshevich. All of them graciously offered an ear for discussion and consolation as well as distractions from the rigors of sciences.

I would also like to thank family and friends outside of graduate school. Millie Milliken, Kari Kendzerski, Lucy Kirchner, Lindsie Goss, and Jennifer Jung in San Francisco willingly offered support, which were vital for my mental and emotional health. I would also like to thank Jessica Gahres for her unwavering support for my scientific endeavors. Her encouragement and belief in my talents as a scientist truly invigorated my commitment to science and graduate school. As for my family, my uncle, Philip York, generated numerous discussions through comments and questions that were both insightful, humbling, and of course humorous. I would also like to thank my parents, Bill and Rosemary, who took a great interest in my scientific and philosophical development and have always had a steadfast commitment to my education. As for my mother, her unrelenting dedication and sacrifices for my accomplishments are a testament of her

unparalleled character. None of this would have been possible without her. Finally, I would like to that my partner in crime, Rob. His unassuming nature and level disposition often counter my fanatical and emotional breakdowns. I'm grateful for his calming influences and judicious advice.

ABSTRACT

Non-receptor protein tyrosine kinase Syk mediates signal transduction pathways downstream of immunoreceptors, integrins, and C-type lectins and is expressed in immune cells. Overexpression and aberrant activation of Syk is observed in numerous hematopoietic malignancies and autoimmunity. These studies examined whether constitutively active versions of Syk lead to deregulated signaling, aberrant function in hematopoietic cells, and generation of hematological malignancies. A previously characterized fusion protein TEL-Syk was analyzed for constitutive activity, hypersensitivity toward low-dose cytokine stimulation and generation of a myeproliferative neoplastic disease. TEL-Syk expressing fetal liver hematopoietic cells led to constitutive activation, induced myeloid expansion/dysmyelopoiesis and dyserythropoiesis, myelofibrosis, elevated circulating inflammatory cytokines and JAK2-independent phosphorylation of STAT5. Therefore TEL-Syk causes a pre-leukemic myeloid disorder rather than a lymphoid leukemia as previously published. We further examined whether Y(342, 346)A mutations within interdomain B of Syk lead to constitutive activation and deregulated signaling. Expression of Syk Y(342, 346)A in 293T cells led to constitutive phosphorylation of NTAL and other tyrosine containing targets, but demonstrated reduced autophosphorylation. Primary macrophages expressing Syk Y(342, 346)A phagocytosed IgG-opsonized SRBCs normally, but failed to mobilize calcium or transform Ba/F3 cells. Lastly, to address whether disruption in auto-regulatory motifs in Syk led to constitutive activation, we generated an allelic series within Syk, then determined the ability of these mutants to phosphorylate the downstream adaptor NTAL following co-expression in 293T cells. Although Syk mutants enhanced overall tyrosine phosphorylation, only Syk mutants W135A and Q149A increased

autophosphorylation. Furthermore, DT-40 B-cells expressing these Syk mutants demonstrated a hypomorphic calcium mobilization response after BCR cross-linking as compared to cells expressing a wild-type Syk, suggesting that other regulatory mechanism may compensate for constitutive Syk activation. We also found that all Syk mutants did not transform Ba/F3 in the absence of IL-3 as compared to TEL-Syk. Our data demonstrates that TEL-Syk is a potent oncogene that drives a myeloproliferative neoplasm with robust myelofibrosis, and disruption of auto-regulatory motifs in Syk lead to constitutive NTAL and tyrosine phosphorylation. These studies provide a system to study deregulated Syk signaling in hematopoietic malignancies and additional evidence to target the kinase domain to treat human leukemias.

TABLE OF CONTENTS

LIST OF FIGURES

CHAPTER ONE

INTRODUCTION

1.1 Hematopoiesis: from stem cell to blood cells

Hematopoiesis is the development of an array of blood cells -- encompassing red blood cells/erythrocytes, thrombocytes, and white blood cells/leukocytes -- from stem cells that reside in bone marrow niches. These early stems cells have the capacity to undergo self-renewal and subsequent differentiation to give rise to a full complement of the blood system as demonstrated by chimeric mouse studies involving isolation and serial transplantation of pluripotent stem cells into lethally irradiated recipients (Ross et al., 1982; Till and McCulloch, 1961). These stem cells go through a series of differentiation steps, known as cell lineage commitment, to terminally differentiate into a mature blood cell (Weissman et al., 2001). Long-term hematopoietic stems or LT-HSCs are the most pluripotent of the stems cells and exist in a quiescent stage, replicating ~every 8 days in mice and 40 weeks in humans (Catlin et al., 2011; Passegue et al., 2003). LT-HSCs undergo a differentiation step to give rise to short-term hematopoietic stem cells, ST-HSCs, which still possess self-renewing properties but have faster proliferative capacity (Catlin et al., 2011; Passegue et al., 2003). ST-HSCs then give rise to multipotent progenitors (MPPs) that can repopulate an irradiated recipient with mature blood cells, but not LT-HSCs or ST-HSCs; thus, demonstrating that MPPs have lost a small degree of plasticity compared to LT-HSCs and ST-HSCs. From the MPP stage, cells deterministically become two separate lineages: common myeloid progenitors (CMPs) or

common lymphoid progenitors (CLPs) (Iwasaki and Akashi, 2007). CMPs give rise to both myeloid, which encompasses granulocytes (neutrophils, eosinophils, basophils), monocytes/macrophages, mast cells, myeloid-derived dendritic cells, and erythroid cells (thrombocytes/platelets and red blood cells/erythrocytes) (Iwasaki and Akashi, 2007; Wu and Liu, 2007). Myeloid lineage commitment is largely dependent on a group of circulating cytokines termed colony-stimulating factors, which exert effects on CMPs to become granulocytes and monocytes/macrophages. These factors (GM-CSF, G-CSF, and M-CSF) as well as interleukin (IL)-3, -6, -1, -11, c-kit, thrombopoietin (TPO), erythropoietin (EPO) and stem cell factor (SCF) are some of the main cytokines that direct myeloid and erythroid development (Iwasaki and Akashi, 2007; Lotem and Sachs, 2002; Ogawa, 1993; Sun et al., 2006). Lymphocytes such as B-cells, T-cells, natural killer (NK) cells, NKT cells, and lymphoid-derived dendritic cells (DCs) evolve from the CLP and are chiefly maintained by the cytokine interleukin-7 (Iwasaki and Akashi, 2007; Rothenberg, 2007). Notch-Delta signaling, a cell-membrane bound regulator, found in the bone marrow microenvironment deterministically dictates early T-cell fates (Rothenberg, 2007). Cell fates are influenced by the bone marrow microenvironment and circulating cytokines, which in turn drives the complex orchestration of signaling pathways and transcription factors (which are beyond the scope of this dissertation) (Metcalf, 2007; Rothenberg, 2007); further diversifying the cellularity within the bone marrow and ultimately contributes to the generation of mature blood cells.

1.2 Temporal locations of hematopoiesis

In mammals, hematopoiesis begins in the yolk sac, composed mainly of erythro-myeloid progenitors, and then is found in the aorta-gonad-mesonephros (AGM) region during

organogenesis (Adams and Scadden, 2006; Boisset and Robin, 2012; Costa et al., 2012). In the AGM region and then the Para-aortic Splanchoneopleura (P-Sp) region hemiangioblasts are present, revealing an intimate association between the blood system and vascular stromal and endothelial cells. Lymphoid precursors emerge within the AGM and P-Sp regions, where B- and T-cell progenitors were discovered based on colony-forming assays of AGM and P-Sp tissues grown on S-17 stromal cells and fetal thymic organ culture respectively (Boisset and Robin, 2012). Lymphoid progenitors are also found within the yolk sac at these later stages of development. After proper vascularization, hematopoiesis localizes to the fetal liver by mid-gestation and HSCs undergo rapid expansion. By late gestation and bone mineralization, HSCs migrate and colonize the long bones and form close association with osteoclasts and stromal cells that reside in and support the bone marrow microenvironment. HSCs in the bone marrow microdomains, or niches, slow in cell-cycling and becoming quiescent. Through cell-cell contacts and interactions with extracellular matrix proteins, soluble cytokines and chemokines, bone marrow niches maintain HSCs in a quiescent state. Most notably Kit ligand, Notch1 ligand Jagged, CXCL12, VCAM-1 and angiopoetin-1 on stromal cells are necessary for HSC maintenance (Levesque and Winkler, 2011). As stated above, necessary differentiation cues within subregions of the bone marrow microenvironment dictate cell lineage commitment and blood cell development. The highly vascularized nature of the bones enable HSC migration in and out of the bone marrow niches and eventual colonization of small bones, such as the ribs and sternum, as the mammal ages. Disruption of bone microenvironments by deletion of stromal progenitors lead to myelodysplasia with an increased risk to leukemic transformation, revealing the

importance of the bone marrow microenvironment in HSCs maintenance (Raaijmakers et al., 2010).

1.3 Myeloproliferative Neoplasms

In 1951, William Dameshak coined the term myeloproliferative disorders or MPD to describe a spectrum of blood disorders that encompasses pre-leukemic and leukemic conditions (Tefferi, 2008). Advances in cytology promoted the discovery of chromosomal abnormalities or lesions association MPDs, most notably the Philadelphia chromosome (Ph^+) in chronic myelogenous leukemia (CML) that was discovered in 1960 by Peter Nowell in collaboration with David Hungerford (Tefferi, 2008). Subsequent studies by Fialkow et al. established that these blood disorders are clonal, or derived from a single cell with a cancer-initiating event, and hematopoietic in origin based on linkage of glucose-6-phosphate polymorphisms found in proliferating Ph^+ blood cells (Tefferi, 2008). In 1973, the field took a giant step in elucidating the causative elements in MPDs with the discovery of the BCR-ABL fusion due to a chromosomal translocation associated with CML, which is currently used as a biomarker for Ph^+ CMLs (Rowley, 1973). These series of key studies established that MPDs are clonal blood disorders arising from the bone marrow and are often accompanied by a genetic lesion that plays a major role in disease progression.

In 2008, the World Health Organization reorganized the MPD field under myeloproliferative neoplasms or MPNs to describe and to encompass not only myeloproliferative conditions, but also some myelodysplastic disorders (Fig 1.1) (Vardiman et al., 2009). These neoplasms were of granulocyte, monocyte/macrophage, erythroid, megakaryocyte and mast cell origins and with the presence of 20% blasts, or

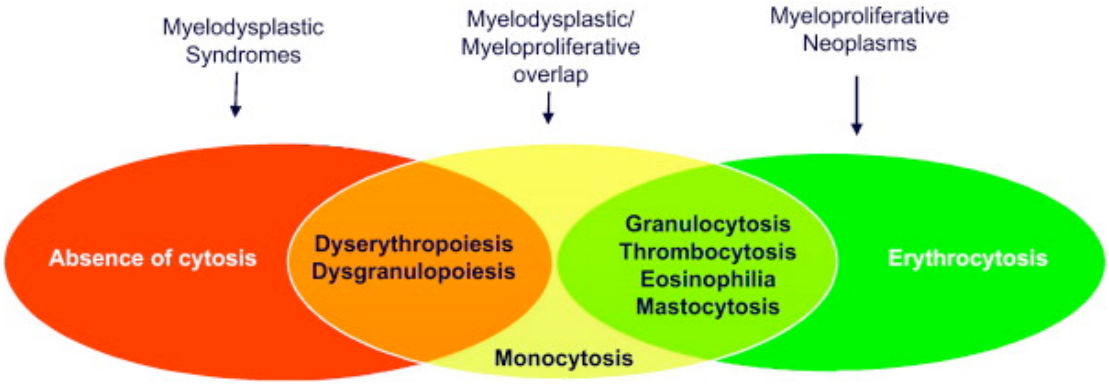

Figure 1. 1 2008 WHO classification of chronic myeloid malignancies (Tefferi, 2012)

expansion of blood cells with a block in differentiation, where considered to have progressed to acute myeloid leukemia (Klampfl, 2011). In addition to immunophenotypic, morphological, cytogenetic, and clinical features, classification of these disorders were largely based on rapidly emerging genetic evidence for correlative and/or causative lesions.

1.4 Genetic lesions lead to deregulated signaling and leukemogenesis

The 2008 WHO classification of MPNs highlighted several key mutations in transmembrane and cytoplasmic kinases, most notably *Janus Kinase 2* (JAK2*) V617F* in 90% of polycythemia vera (PV), 50% of primary myelofibrosis (PMF) patients and a few cases of essential thrombocythemia (ET). Myeloproliferative leukemia virus oncogene (MPL/thrombopoietin receptor) *W515L* is an additional mutation that correlates with ET in *JAK2 V617F* patients (Vardiman et al., 2009). These mutations activate tyrosine kinase function, conferring cytokine hypersensitivity/independence, and recapitulate the human disease in mouse models either through retroviral transplantation assays or transgenic/knockin models (Vainchenker et al., 2011). *JAK2V617F* leads to progressive

anemia, splenomegaly, myelo-expansion, and fibrosis of the bone marrow. This mutation disrupts autoinhibition of JAK2 and drives deregulated signal transduction pathways downstream of multiple cytokine receptors (Quintas-Cardama et al., 2011). These mutations as well as other chromosomal translocation -- *TEL-ABL*, *TEL-JAK2, FLT3/ITD* in acute myeloid leukemia (Klampfl, 2011) and acute lymphocytic leukemia (ALL); *ETV6-PDGFRB* (TEL-PDGFRB) in chronic myelomonocytic (CMML); *FIP1L-PDGFRA* in chronic eosinophilic leukemia -- yield constitutively active kinases that lead to deregulated signaling (Holroyd et al., 2011). Novel mutations in *IDH*, *EZH2*, *TET2*, *IKZF1*, *ASXL1*, *CBL* have recently been identified in a number of MPNs. The exact role of these various mutations in deregulated signaling is unknown, but an increased risk of leukemic transformation from MPN to AML has been associated with either the loss of tumor suppressor function as in the case of *CBL* and *IKZF1*, or promotion of blast formation as in the case of *TET2*, *IDH*, and *EZH2*; in the case of *ASXL1*, either loss of tumor suppressor function or deregulated retinoic acid signaling may contribute to leukemic transformation (Tefferi, 2010).

The signal transducer and activator of transcription (STAT) family of signal transduction mediators are largely involved in manifesting such deregulated signaling. Of these STATs, STAT5 plays a major role in transmitting signals from a number of cytokine receptors and associated kinases, such as MPL and JAK2, for cellular survival. Upon JAK2 and MPL activation, proximal STAT5 becomes phosphorylated and translocates the nucleus to initiate transcription of hematopoietic lineage genes such as *Pim1, Bclx, and Socs2* (Murray, 2007). Deficiencies in STAT5 abrogate the disease phenotypes generated in the TEL-PDGFRB (Cain et al., 2007), TEL-Lyn, JAK2V617F

and BCR-ABL mutant mice thus, revealing a predominant role for STAT5 in the MPN pathogenesis (Hantschel et al., 2012; Takeda et al., 2011; Van Etten, 2002).

1.5 Predictive power of proinflammatory cytokines in MPN

Recent studies examining serum from patients and mouse models of MPNs found a pro-inflammatory cytokine signature. In PMF patients sera proinflammatory cytokines IL-13, -8/CXCL8, -2R, -12, -15, TNFα, G-CSF, MIP-1α/CCL3, MIP-1β/CCL4, IP-10, MIG, MCP-1/CCL2, IP-10/CXCL10 are increased, while IFNγ is decreased. Of the inflammatory cytokines analyzed, IL-1RA, -2R, -6, -8, -12, MIP-1a, IP-10, and MIG correlated with reduced survival and *JAK2V617F*$^{+}$ PMF patients correlated with increased IL-1RA, -2R, -6, -12, HGF, IP-10, and MIG (Tefferi et al., 2011). Both IL-8 and IL-2R were deemed risk factors for disease severity and survival, in which higher levels of either or both of these cytokines results in reduced survival (Tefferi et al., 2011). The authors suggest that increased inflammatory cytokines, especially IL-8 and IL-2R, promote an inflammatory state that further alters hematopoiesis and exacerbates cachexia and underlining cardiovascular conditions. Furthermore, inflammatory cytokine signatures are found in PV patients, in which IL-1RA, -5, -6, -7, -8, -12, -13, IFNγ, GM-CSF, MIP-1α, MIP-1β, MCP-1, MIG and VEGF were increased and IL-1β, -4, -5, -7, -10, -17, EGF, IFNα, TNFα, GM-CSF, MIP-1α, MIP-1β, and MCP-1 correlates with reduced survival (Vaidya et al., 2012). Finally, patients with myelodysplastic syndrome (MDS) were evaluated for a panel of inflammatory plasma cytokines. The analysis revealed that IP-10, IL-7, and IL-6 were poor prognostic factors for survival. MCP-1, MIG, G-CSF, TNFα, IL-13, -8, -15, IFNγ, and HGF were also significantly increased but were not analyzed for disease severity or survival (Pardanani et al., 2012). Increase of

these cytokines as well as an array of other inflammatory cytokines also correlated with PMF, demonstrating that an inflammatory cytokine signature is a common hallmark of MPN with predictive power for both disease severity and survival.

1.6 Non-receptor tyrosine kinase structure and function

Tyrosine kinases, enzymes that post-translationally modify proteins with the addition of phosphate groups, fall into two categories of signaling proteins, receptor protein tyrosine kinases (RTK) and non-receptor protein tyrosine kinases (NRTK). These enzymes integrate soluble extracellular signals to regulate cell proliferation, differentiation, survival, cytoskeletal rearrangment, cell cycle control and metabolism (Lemmon and Schlessinger, 2010). RTKs consist of an extracellular ligand binding domain, a transmembrane-spanning helix, and a cytoplasmic kinase domain. Within the kinase domain, there are two lobes, N-terminal and C-terminal, and an activation loop, which is composed of one to three tyrosines and enables the transfer of phosphate groups to downstream substrate/target proteins. The N-terminal lobe contains five-stranded β sheets with one α-helix, while C-terminal contains several α helices, which generate a substrate-binding pocket. Linking the two lobes is the activation loop that contains an ATP binding cleft and tyrosines for phosphotransfer. Within the third β sheet of the N-terminal lobe, a lysine, which is highly conserved between all kinases, stabilizes ATP molecules within the ATP binding pocket and is necessary for catalytic function. Several glycines in the ATP binding site, an aspartic acid and asparagine in the activation loop and a glutamic acid in the α-helix C of the C-terminal lobe are also highly conserved and necessary ATP stabilization and catalysis (Johnson et al., 1996). RTK often exist as monomers, but upon ligand cross-linking RTKs non-covalently dimerize and lead to phosphorylation of

downstream target proteins by transferring a phosphate groups from an ATP molecule on to a reactive residue on the target protein.

NRTKs are cytoplasmic and often contain domains, Src homology 2 (SH2) and 3 (SH3), that dock on to phosphotyrosines on activated cell surface receptors or coupled-adaptors. Phosphotransfer regions, motifs in between the kinase lobes, are relatively conserved and phosphorylate proteins similarly among RTKs and NRTKs. For intracellular signaling proximal to the plasma membrane, Src-family kinases are post-translationally modified, by palmitoylation or myristoylation, and insert into the plasma membrane (Hubbard and Till, 2000), while Tec family kinases link to the plasma membrane through pleckstrin homology (PH) domain, which bind to phosphatidylinositol lipids present at the plasma membrane. The Jak family, Jak 1, 2, 3 and Tyk2 kinases, bind to activated cytokine receptors through Jak homology domains, which are unique to this family of NRTKs, and enable STATs dimerization and translocation to the nucleus for gene expression.

Autophosphorylation, or the ability for the kinase to transfer phosphate groups to intrinsic tyrosines, is an integral step in both RTKs and NRTKs activation. Receptor dimerization upon ligand binding or docking SH2 or SH3 domains to phosphorylated adaptors leads to conformational changes in the kinase that induces *cis*-autophosphorylation (within the kinase), while activation of neighboring kinases lead to *trans*-phosphorylation (between kinases); both *cis*- and *trans*- autophosphorylation lead to subsequent kinase activation (Fig. 1.2 A). Autophosphorylation of activation loop tyrosines is optimal for substrate binding and catalysis, as these phosphotyrosine stabilize the activation loop in an open configuration, while autophosphorylation of other tyrosines

scattered through out the kinase is necessary for recruitment of downstream signaling targets and regulation (Hubbard and Till, 2000; Johnson et al., 1996; Lemmon and Schlessinger, 2010).

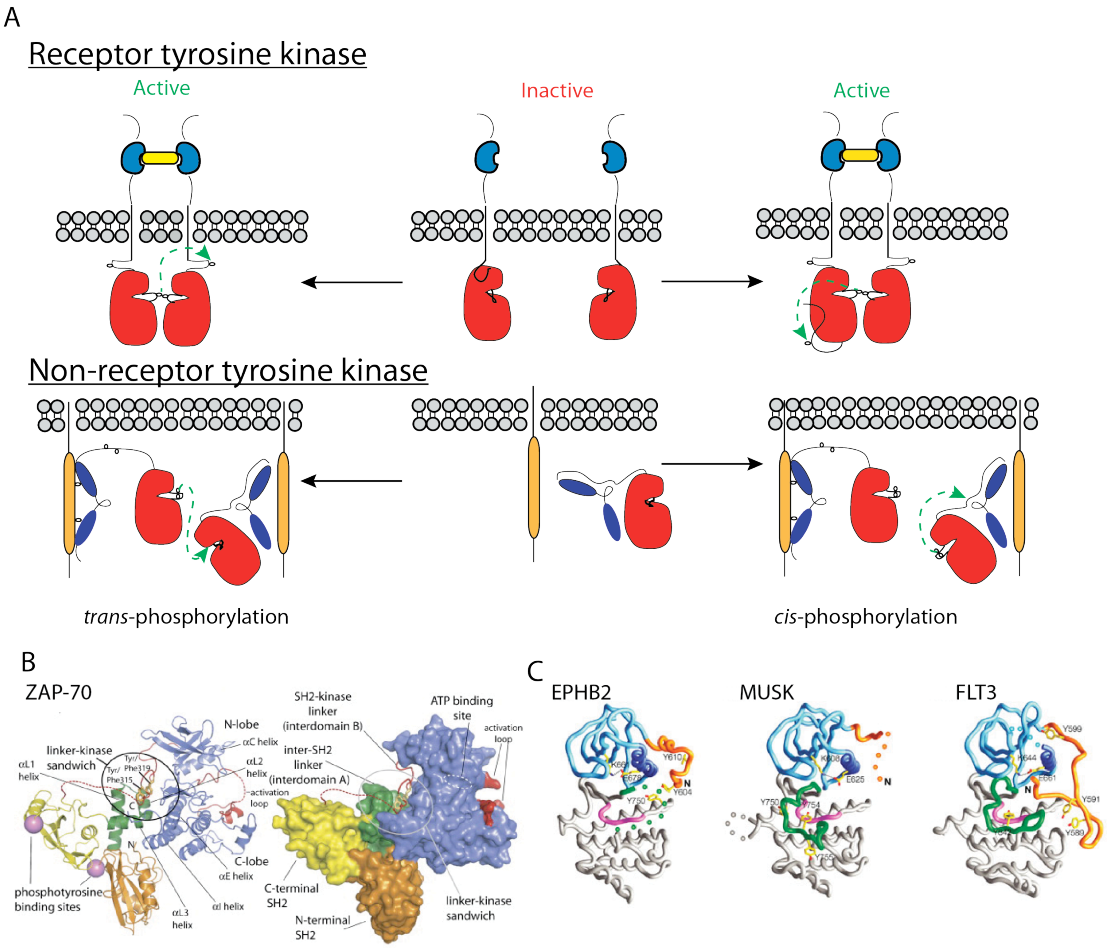

Figure 1. 2 Modes of receptor and non-receptor tyrosine kinase activation and autoinhibition (A) schematic of *cis*- and *trans*-phosphorylation of receptor (upper panel) and non-receptor (lower panel) tyrosine kinase phosphorylation. In the upper panel, the blue domains represent the extracellular ligand binding domain, while in the lower panel the blue domain depict intracellular protein-to-protein binding domains.The yellow bands depict the ligand (upper panel) and adaptor proteins (lower panel) and the kinase domain is depicted in red in both the receptor and the non-receptor tyrosine phosphorylation schematics (Hubbard, 2004). (B) Ribbon structures for inactive non-receptor tyrosines kinases. The kinase domains of ZAP-70 are depicted in blue, while the SH2 protein binding domains are depicted yellow. The activation loop is featured in red (Deindl et al., 2007). (C) Juxtamembrane (orange) autoinhibition of receptor tyrosine kinases. The N-terminal lobes of the kinase domain are depicted in light blue; C-terminal lobes of the kinase domain are colored in grey; the activation loop is colored in pink and the activation segment is color in green (Hubbard, 2004).

Mechanisms of autoinhibition vary among tyrosine kinases and depend on regulatory domains that are either proximal or distal to the activation loop. These regulatory regions maintain an autoinhibited conformation by interacting with residues in the kinase domain, with other regulatory domains or with other proteins. For example, non-receptor tyrosine kinase ZAP-70 makes a linker-kinase sandwich, in which a regulatory linker region and the C-terminal lobe of the kinase domain occlude key tyrosine residues within interdomain B (Fig. 1.2 B) to maintain an inactive conformation. Juxtamembrane motifs within the Ephrin and MUSK families of receptor tyrosine kinases allosterically occlude ATP from the ATP binding sites (Fig. 1.2 C), while the juxtamembrane loop of FLT3 interacts with the two lobes of the kinase domain to maintain a closed and inactive confirmation. Key tyrosines in these regulatory regions (e.g. linker domains of ZAP-70 and juxtamembrane motifs of Ephrin, MUSK, and FLT3) are necessary for autoinhibition, and autophosphorylation of these residues relieves autoinhibition thus, enabling kinase function. Modes of autoinhibition include preventing activation loop tyrosine phosphorylation for proper activation loop stability, occluding substrate and ATP access to the phosphotransfer site, and other allosteric interactions within the kinase domain or between regulatory domains (Hubbard, 2004; Lemmon and Schlessinger, 2010). After receptor ligation tyrosine kinases are either *cis*- or *trans*-phosphorylated at the activation loop tyrosines, which promote movement of the activation loop into an open conformation. Subsequent *trans*-phosphorylation of other regulatory tyrosines disrupts intramolecular inhibitory interactions and enables optimal kinase activation. Mutations of key regulatory residues lead to deregulated signaling by phosphorylating a plethora of downstream target proteins and inappropriately inducing

cell activation and proliferation. For example, *JAK2V617F* enables constitutive activation of Jak 2 by disrupting autoinhibitory intramolecular interactions between the JH2 pseudokinase domain and JH1 kinase domain, thereby deregulating cytokine receptor signaling that is intergral in hematopoiesis and immune responses (Quintas-Cardama et al., 2011).

1.7 The role of Syk in immune receptor signal transduction

Spleen tyrosine kinase (Syk) is a NRTK that mediates signal transduction from a variety of immunoreceptors, integrins, and C-type lectins (Mocsai et al., 2010). Syk was initially identified from a porcine spleen expression library through its high degree of homology to zeta-associated protein (ZAP-70), another NRTK that signals downstream of the T-cell receptor (TCR). Both Syk and ZAP-70 contain two SH2 domains at the N-terminus and kinase domain at the C-terminus (Fig. 1.3 A). Syk is expressed in a variety of hematopoietic and epithelial cells, where it mediates cellular activation, cytokine production, survival, cell adhesion, and degranulation (Sada et al., 2001). Deficiency in Syk disrupts B-cell development at the pro-B cell stage and is necessary for proper B-cell receptor (BCR) signal transduction (Turner et al., 1995). Syk is necessary for integrin- and Fc-mediated phagocytosis and effector functions in macrophages and neutrophils, mediating activating-receptor effector function in NK cells, fungal immunity through CLEC7A/Dectin-1, platelet activation via GPVI, and osteoclast maturation (Mocsai et al., 2004; Mocsai et al., 2002; Turner et al., 1995). Palacios et al. demonstrated that Syk also plays a minor role in thymocyte development, where deficiency in Syk leads to impaired pre-TCR signaling and reduced cell cycle entry at the DN3 stage (Palacios and Weiss, 2007).

Upon immunoreceptor ligation Src-family kinases (SFK), which are tethered to lipid rafts and proximal to the immunoreceptors, phosphorylate tyrosines in the $D/EX_2YXXL/IX_{7\text{-}10}$ motif, or immuno-receptor tyrosine-based activating motifs (ITAMs), located on adjacent adaptors, such as Igα/Igβ, DAP12 and FcRγ (Fig. 1.3 B). Doubly phosphorylated ITAMs within the adaptors provide a docking site for the two SH2 domains in Syk, which facilitates either Src-mediated phosphorylation or Syk autophosphorylation, allowing Syk to unfurl into an open and active conformation. Proximal to both membrane-tethered adaptors and other scaffold and signaling proteins, Syk phosphorylates NTAL/LAB, SLP-76/BLNK, Vav, PLC-γ, and other signaling molecules to propogate signals through to the MAPK, PKC, IP_3, and PI3K pathways for cellular activation (Mocsai et al., 2010). Furthermore, Syk plays an antagonistic role in innate immune responses by dampening Toll-like Receptor (TLR) responses upon microbial byproduct stimulation. Downstream of DAP12-associated receptors, TREM-1 and -2, Syk not only reduces pro-inflammatory cytokines TNFα, IL-6, and IL-12, but also upregulates anti-inflammatory cytokine IL-10 after CpG, Zymosan, and LPS stimulation of TLRs (Hamerman et al., 2005).

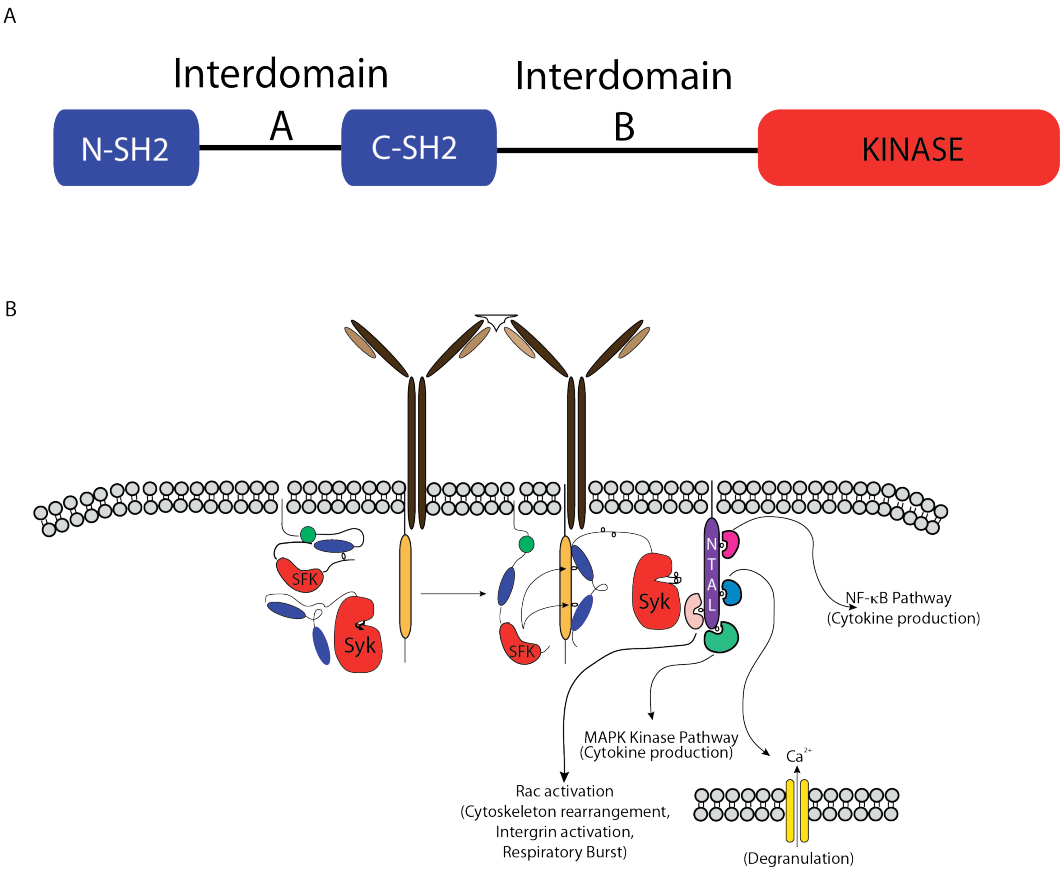

Figure 1. 3 Syk mediates immunoreceptor signal transduction and cellular activation (A) Schematic of Syk protein binding domains (SH2 in blue), kinase domain (red), and regulatory interdomains A and B (B) BCR engagement (brown ovals) by cognate antigen (white polygon) activates Src family kinases and Syk. SH2 domains (blue oval) bind to doubly phosphorylated ITAM-containing adaptors (yellow) and phosphorylate downstream adaptor NTAL (purple oval) to initiate multiple cellular responses.

1.8 A Syk conundrum: role of Syk as both an oncogene and tumor suppressor.

Syk has been implicated in a number of hematopoietic, lymphocytic, and epithelial cancers as a proto-oncogene. Gene-expression profiles studies revealed Syk over-expression in B-lymphoproliferative disorders (Waldenstrom's macroglobulinemia) (Gutierrez et al., 2007), mantle cell lymphoma (Rinaldi et al., 2005), diffuse large B-cell lymphoma (DLBCL) (Monti et al., 2005), peripheral T-cell lymphoma (PTCL) (Feldman et al., 2008) and chronic lymphocytic leukemia (CLL) (Buchner et al., 2009). The results championed the potential of Syk as a therapeutic target and CLL prognostic factor. As a downstream mediator of BCR cell activation, Syk enables B-cell lymphoma and

leukemic cell survival; administration of the Syk inhibitor R406 reduces STAT4 and ERK phosphorylation in primary CLL cells and induces apoptosis in both primary CLL cells and DLBCL cell-lines (Chen et al., 2008). Furthermore, administration of Syk inhibitor R406 to AML cell-lines has revealed a novel role of Syk as a modulator of AML dedifferentiation, in which shRNA knockdown or R406 treatment induce HL-60 and U937 cells to differentiate into morphologically and immunophenotypically mature myeloid cells (Hahn et al., 2009). Further supporting the role of Syk as oncogene, several fusion proteins, TEL-Syk (Kuno et al., 2001) and ITK-Syk (Streubel et al., 2006), containing the C-terminus kinase of Syk lead to lymphomas and MPN/MDS in humans.

In contrast, Coopman et al. elegantly demonstrated that Syk retains a tumor suppressive function in mammary epithelium and prevents breast cancer severity and invasiveness such that at advanced stages of breast cancer Syk is undetectable and unable to suppress invasive outgrowth (Coopman et al., 2000). Moreover, deficiency in Syk correlates with poorer prognosis in breast cancer patients (Moroni et al., 2004; Toyama et al., 2003). In mouse mammary epithelium, Syk suppresses ductal branching and proliferation and deficiencies in Syk leads to hyperplasia and tumor formation (Sung et al., 2009). Epigenetic silencing of Syk expression has been documented in various other epithelial derived cancer notably melanoma (Bailet et al., 2009; Muthusamy et al., 2006), pancreatic ductal adenocarcinoma (Layton et al., 2009), and lung cancer (Dong et al., 2011), whereby loss of Syk promotes anchorage-independent cell growth, dedifferentiation, and invasion. Thus, the antithetical role of Syk as either a proto-oncogene or a tumor suppressor underscores the complex biology of Syk and the significance of cell context.

CHAPTER TWO

MATERIAL AND METHODS

2.1 Mice

BALB/c (CD45.2) and BALB/c.SJL (CD45.1) mice were purchased from Taconic Laboratories and bred in the animal facility at UCSF. Experiments were conducted in compliance with the UCSF Institutional Animal Care and Use Committee specified guidelines.

2.2 Cells

HEK 293T cells were cultured in Dulbecco's Modified Eagle's Medium (DMEM) supplemented with 10% fetal bovine serum (FBS) (v/v) and 100μg/mL penicillin/100U/mL streptomycin. Fetal liver cells from 16-19 days post-coital (dpc) pregnant BALB/c mice were isolated and cultured overnight in Iscove's Modified Dulbecco's Medium (IMDM) supplemented with a cytokine mix consisting of 10ng/mL of murine IL-6, 20ng/mL of murine IL-3, and 100ng/mL of murine SCF (R&D Systems) and 15% (v/v) FBS for reconstitution of irradiated recipient mice. For CFU-colony assays, isolated fetal liver cells were cultured in IMDM supplemented with IL-3, IL-6, SCF at the above concentrations, plus 10ng/mL of IL-11, and 10ng/mL of Flt3L (R&D Systems).

2.3 Plasmid and retroviral transduction

Retroviral supernatants were generated using a method previously described (Mocsai et al., 2006). The retroviral expression vector pMIG-W, possessing an internal IRES-GFP for marking of infected cells, contained either murine Syk, human TEL-Syk or human TEL-Syk kinase dead (KD), with human TEL-Syk kindly provided by Dr. Hassan Jumaa. TEL-Syk KD and Syk allelic series were generated using the Quikchange site-directed mutagenesis kit (Stratagene) using primers (Sigma-Aldrich) containing amino acid alterations (Fig. 4.2 A and B)

For transduction of retroviral constructs, 5-7 x 10^6 purified fetal liver cells were spin-infected in DMEM supplemented with 15% FBS, 8μg/mL of polybrene (Sigma), and 1X IL-3, IL-6, and SCF (at the above concentrations) by centrifugation at 2000 rpm for 1 hour at 25°C in viral supernatant. Cells were then placed at 37°C overnight. Transduced fetal liver cells were washed the next day and placed in 15% FBS IMDM with indicated cytokines. Retroviral infection efficiency was determined by flow cytometry to assess GFP expression.

2.4 CFU-Colony Assays

BALB/c fetal liver cells were isolated at 16-19 dpc and transfected with vector, Syk, TEL-Syk and TEL-Syk KD. GFP^+ cells were sorted using the FACS Aria (BD Bioscience) and plated at a density of 2 x 10^4 in methylcellulose (StemCell technologies), according to manufacturer's directions, with 1ng/ml IL-3, 1ng/ml IL-6, and 5ng/ml SCF, which is indicated as the 1X concentration in Fig. 1. Plating was also done at 0.1 and 0.01X cytokine concentrations and cells were cultured for 12 days, then colony numbers counted in phase microscopy. Cells were washed from the plates with IMDM containing

2mM EDTA, collected, and counted by trypan blue exclusion to obtain total cell numbers.

For JAK inhibition studies, sorted GFP^+ cells were plated at a density of 2×10^4 in methylcellulose in the presence of 10ng/mL GM-CSF (Peprotech) and varying concentrations of JAK inhibitor 1 (EMD Millipore). After 7 days in culture, plates were enumerated in phase microscopy.

2.5 Immunoblots and immunoprecipitation

For NTAL phosphorylation, HEK293T cells were washed in cold PBS with 1mM Na_3VO_4 and treated with RIPA buffer (20mM Tris pH 7.5, 150mM NaCl, 1% Triton X-100, 1% Na-DOC, 0.1% SDS) containing protease inhibitors (1mM Na_3VO_4, 50mM NaF, 2mM EDTA, 1mM Pefabloc, 10g/ml of leupeptin, 2g/ml of aprotinin, 1mM dithiothreitol, 1g/ml of pepstatin and 1mM di-isopropyl fluorophosphate). Cell lysates were pelleted and cell supernatants were treated with sample buffer prior to boiling and SDS-PAGE separation. Proteins were transferred to Immobilon PVDF membranes (Millipore) and were detected by anti-Syk antibodies (Cell Signaling, cat#: 2712) for TEL-Syk and Syk, anti-NTAL (Cell Signaling), p-Tyr (4G10, Upstate Technologies), phospho-STAT5 and STAT5 (14H2 and 3H7 Cell Signaling), anti-Erk1/Erk2 (Santa Cruz Biotech), and anti-GFP (Novus).

For the *in vitro* kinase assay, methods were as previously described (Mocsai et al., 2006). In brief, HEK 293T were washed and lysed as above, with a small volume set aside for whole cell lysate analysis. Cell lysates were immunoprecipitated with anti-Syk and protein-A or G sepharose beads (GE Healthcare). Immunoprecipitates were split into two,

with one set washed in kinase buffer (20mM Hepes ph 7.4, 10mM $MgCl_2$, 2mM $MnCl_2$, 1mM dithiothreitol) and then supplemented with 5μCi γ-ATP (Perkin Elmer) for 20 minutes at 25°C. Radioimmunoprecipates were separated by SDS-PAGE and stained with Coomasie blue. Gels were then vacuum-dried and exposed to BioMax (Kodak) autoradiograph film. The remaining immunoprecipitates were treated with sample buffer and separated by SDS-PAGE. TEL-Syk and Syk were detected by anti-Syk and p-Tyr by 4G10.

For analysis of phospho-STAT5 and total STAT5 from sorted fetal liver, GFP^+ cells were collected and washed several times in PBS. Cells were treated with 4X sample buffer with a final concentration of 5 $x10^6$/mL in 1X sample buffer. Equal volumes of lysates were loaded on to a 4-20% gradient SDS-PAGE gel, transferred to immobilon membranes and incubated with anti-phospho-STAT5 and anti-STAT5, anti-Erk1/Erk2, and anti-GFP.

For analysis of total phosphotyrosine, and Syk in tissues from mice receiving vector or TEL-Syk transduced cells, 5 $x10^5$ splenocytes and bone marrow cells are washed 2 times in PBS to remove excess FBS and treated with sample buffer. Cell lysates are separated by SDS-PAGE, transferred to immobilon membranes and incubated with anti-Syk, anti-Erk1/Erk2 and anti-GFP antibodies. Mouse- and rabbit- raised primary antibodies were detected by IRDye secondary antibodies and imaged using the Odyssey Infrared Imaging system (LI-COR biosciences).

2.6 Generation of radiation chimeric mice

Two-three month old BALB/c recipient mice were lethally irradiated with 1200 rads (dosed as 600 rads, twice separated by 3 hours between exposures). For each recipient, 5 x 10^6 cells of virally transduced cells were retro-orbitally injected and recipients were placed on antibiotics for 21 days. Assessment of reconstitution and incorporation of retroviral constructs was assessed by retro-orbital collection of peripheral blood for analysis of the linked GFP marker.

2.7 Peripheral blood analysis

Peripheral blood was collected in an EDTA-treated microtainer (BD Bioscience) for complete blood count (CBC) analysis and in PBS with 2U/mL of heparin for flow cytometry. Heparinized peripheral blood was centrifuged and treated with ACK lysis buffer (BD Biosciences) twice to remove red blood cells. Purified peripheral blood was incubated on ice with anti-CD16/CD32 (2.4G2; UCSF) and mIgG (Sigma-Aldrich) prior to staining with a cocktail of APC-conjugated, PE-conjugated, and APC-Cy7-conjugated immunomarkers: CD11b (M1/70), Ly6G (1A8), TCRβ (H57-597), CD19 (ID3), NKp46 (9E2), Siglec-F (E50-2440; all from BD Bioscience or eBioscience); F4/80 (Serotec). Cells were washed, resuspended in FACS buffer with 1μg/mL propidium iodide (Sigma) and flow cytometry was performed on a FACScan (BD Bioscience). Data were analyzed using the flow cytometric software FlowJo (Tree Star Inc.).

For CBC analysis, EDTA-treated peripheral blood was analyzed for leukocyte counts and percentages as well as red blood cell numbers and parameters by the HEMAVET (Drew Scientific) machine. The NucleoCounter (Chemometec) was used to enumerate peripheral blood counts.

2.8 Tissue staining and immunohistochemistry

Sternums, livers, and spleens were placed in formalin and paraffin-embedded prior to staining. For histology, sections were treated with hematoxylin and eosin (H&E). Liver and spleen sections were treated with Masson Trichrome for collagen deposition and sternum sections were stained with silver stain for reticulin fibers. For apoptosis analysis, sections were stained with activated cleaved Caspase-3 antibodies (Cell Signaling).

2.9 phospho-STAT5 intracellular staining

Fetal liver cells isolated between 14-18 dpc were cultured in media containing cytokines and then transduced with retroviral vectors as described above. Cells were incubated in media containing cytokines for three days at 37°C. On day 3, cells were starved of cytokines for 6 hours in 1% FBS (v/v) in IMDM and aliquots of cells were collected. After starving, the remaining cells were re-stimulated with 10ng/mL of murine IL-6, 20ng/mL of murine IL-3, and 100ng/mL of murine SCF. All time points were washed and then incubated with 2% (v/v) paraformaldehyde for 15 minutes at room temperature. Cells were pelleted and then treated with ice cold 99% (v/v) methanol for 10 minutes. Cells were then washed three times in PBS containing 0.5 % BSA (w/v) and 0.02% (v/v) sodium azide. Cells were incubated with FcBlock (UCSF CCF) and mIgG (Sigma) for 10 minutes on ice and then incubated with phospho-STAT5-Alexa Fluor 647 (47, BD Bioscience), anti-GFP Biotin (5F12.4, eBiosciences) and streptavidin Pacific Orange (Invitrogen). Cells were washed and flow cytometry was performed on the LSRFortessa cell analyzer (BD Biosciences).

For JAK inhibition studies, retrovirally transduced cells were sorted based on GFP expression and starved for 6 hours in 1% FBS (v/v) in IMDM, pretreated with JAK inhibitor 1 for 30 minutes at indicated concentrations and restimulated with 50ng/mL of GM-CSF. Cells were fixed, permeabilized, and incubated with phospho-STAT5 as indicated above.

2.10 Reverse Transcriptase-PCR

RNA was isolated from 1 x 10^5 GFP^+ and GFP^- splenocytes and bone marrow cells using the RNeasy Micro kit (Qiagen) and iScript cDNA Synthesis kit (Biorad) was used to generate cDNA species. For TEL-Syk detection, primers previously described were used to detect TEL-Syk species at an annealing temperature of 60°C for 30 cycles. Gels were scanned on the AlphaImager station (Alpha Innotech).

2.11 Cytokine Analysis

Cytokine Profiler Array and Angiogenesis Array (R&D systems) were incubated with pooled sera from TEL-Syk and vector mice at 30 days, 45 days, and 60 days (near the onset of TEL-Syk morbidity). Blots were scanned and analyzed on the Kodak Digital Science™ Image Station 440CF system (Kodak). Together, these two arrays detected the following cytokines: IL-1a, IL-1b, IL-1ra, IL2, IL4, IL7, IL10, IL12p70, IL23, IL 27, C5a, IP-10, I-TAC, TIMP-1, G-CSF, M-CSF, GM-CSF, sICAM, IFNγ, KC, Rantes, SDF-1, eotaxin, MCP-5, MIP-1α, JE/MCP-1, MIG, I-309/TCA-1, TREM-1, TNFα, ANG, Ang-1, CXCL16, osteopontin, PD-EGFR, CCD26, EGF, PDGF-AA, PDGR-AA/BB, CD105, collagen, HGF, IFGBP-1, -2, -3, and -9, PTX3, CXCL4, MMP-3, -8, and-9, PIGF-1 prolactin, SDF-1α, serpin E1 and F1, thrombospondin-2 and TIMP-1 and -4.

2.12 Calcium Mobilization

DT-40 chicken B-cells were maintained in RPMI containing 10% FBS (v/v) with 100μg/mL penicillin/100U/mL streptomycin and 10mM HEPES buffer. Retroviral supernatants were generated for each Syk mutant and transduced into DT-40 cells, as described above. GFP^+ DT-40 cells were sorted by a FACSAria and maintained in media for several days before being frozen into aliquots. Thawed DT-40 cells were cultured for several days in media and then washed, resuspended to a density of $5x10^7$ in RPMI, and treated with 10μg of 1mg/mL of Indo-1 (Invitrogen), as methods were previously described (Miller et al., 2009). Cells rocked at 1hr at room temperature, while protected from light. Cells were washed, placed on ice and treated with propidium iodine. DT-40 cells were pre-warmed for 3 mins and baseline calcium responses were recorded by UV emission by an LSRII (BD Biosciences). At 30s into the UV emission recording, DT-40 cells were treated with 500ng/mL of chicken anti-IgM (Jackson Immunoresearch) and the calcium response was recorded for another 3 minutes and 30 seconds.

2.13 Phagocytosis of IgG-opsonized Sheep Red Blood Cells

Femurs and tibias from Syk deficient fetal liver chimeras were flushed with PBS and treated with ACK lysis buffer in order to isolate bone marrow cells, as described previously (Miller et al., 2009). To generate bone marrow-derived macrophages, bone marrow was filtered through a 70μm nylon mesh and layered onto a 62% percoll mix to isolate mononuclear cells. Mononuclear cells were then plated overnight on tissue culture dishes to remove fibroblasts and other adherent stromal populations. Non-adherent cells were collected and transduced with retroviral stocks as described above. Sorted GFP^+ cells were then cultured on Valmark dishes in MEM-α containing 10% FBS

(vol/vol) and 100μg/mL penicillin/100U/mL streptomycin with 10% (vol/vol) CMG medium (cultured supernatants from HEK293 cells expressing rM-CSF). After 7 days in culture, bone marrow derived macrophages (BMDM) were gently detached from the low binding Valmark tissue culture dishes and plated in triplicate at $4x10^5$ cells/mL density in 96-well tissue-culture dishes in MEM-α containing 100μg/mL penicillin/100U/mL streptomycin and 0.5% BSA for 1 hour at 37°C as described previously (Miller et al., 2009). To generate IgG-opsonized sheep red blood cells (SRBCs), SRBCs (PML microbiologicals) were washed twice in $DGVB^{2+}$ (2.5mM Veronal (barbital, Sigma-Aldrich), 75mM NaCl, 2.5% dextrose, 0.05% gelatin, 0.15mM$CaCl_2$, and 0.5mM $MgCl_2$) and resuspend in RPMI 1640 media containing 2% FBS (vol/vol). Anti-SRBC (Rockland) was added to the SRBCs at a 1/64 dilution and incubated in the dark at room temperature for 1 hour while rocking. IgG-opsonized SRBC were then washed twice in $DGVB^{2+}$ and resuspended in RPMI containing 2% FBS. After 1hour of incubation, BMDM were washed with MEM-α containing 100μg/mL penicillin/100U/mL streptomycin and 0.5% BSA. BMDM were treated with either media alone, unopsonized and opsonized SRBCs for 1 hour. After IgG-opsonized SRBCs uptake, BMDM were washed with PBS and treated with ACK to eliminate uninternalized SRBCs. BMDM were washed with PBS and lysed with 0.3% SDS and 200μl of diaminobenzidine substrate (Sigma-Aldrich) was added to measure peroxidase activity from internalized SRBCs. Peroxidase activity was incubated at room temperature for 1 hour in the dark prior to absorbance measurement. Using a Spectramax Plus microplate reader (Molecular Devices), 470nm absorbance was measured as a read-out for phagocytosis.

2.14 Ba/F3 Growth Assay

Ba/F3 hematopoietic mouse cells were maintained in RPMI containing 10% FBS (v/v) with 100μg/mL penicillin/100U/mL streptomycin and 10ng/mL of rmIL-3. Retroviral supernatants were generated for each Syk mutant, TEL-Syk, and control vector and transduced into Ba/F3 cells. GFP^+ Ba/F3 cells were sorted by a FACSAria and maintained in media for several days before being frozen into aliquots. Thawed Syk mutant Ba/F3 cells were resuspended in media with IL-3 and culture for prior to growth assays. Syk mutant Ba/F3 cells were washed several times with fresh media without IL-3, resuspended to a density of $2.5x10^5$ cells/mL with fresh IL-3-deficient media, and plated in triplicates. Cell numbers were assessed every two days by Vi-CELL (Beckman Coulter) cell viability analyzers.

2.15 Statistical Analysis

Parametric and statistical analysis was performed using statistical and graphical software Prism (Graphpad). One-way ANOVA was performed on peripheral blood over 3 months, CFU assays, phospho-STAT5, JAK2 inhibition studies, and at endpoint based on TEL-Syk morbidity for 4 genotypes.

CHAPTER THREE

TEL-SYK LEADS TO RAPIDLY FATAL MYELOFIBROSIS IN MICE

3.1 INTRODUCTION

Chromosomal translocations that result in Syk being fused to other proteins have been isolated in patients with peripheral T-cell lymphoma (Streubel et al., 2006) and MDS where Syk is fused to the non-receptor tyrosine kinase ITK or the transcriptional repressor TEL respectively (Kuno et al., 2001; Streubel et al., 2006). The ITK-Syk fusion protein consists of the PH domain of ITK, a Tec family tyrosine kinase necessary for T-cell development and function (Andreotti et al., 2010), fused with the kinase domain of Syk. When expressed in mouse hematopoietic stem cells, this protein produces a T-cell lymphoma in mice, phenocopying the human disease (Dierks et al., 2010). Ablation of either the PH domain of ITK or the kinase domain of Syk blocks transformation *in vitro* (Rigby et al., 2009).

TEL, or also known as ETV6, is a transcriptional repressor and is necessary for establishing definitive hematopoiesis (Bohlander, 2005; Meester-Smoor et al., 2011). TEL has been implicated in various hematological malignancies, usually as a result of its fusion to various tyrosine kinases, including acute myeloid leukemia, myelodysplasia (MDS), and MPNs (Bohlander, 2005; Holroyd et al., 2011). Of these TEL/PTK fusions, *TEL-Syk* is a rare oncogene isolated from a patient with MDS with a megakarocyte blast and consists of the N-terminal pointed (PNT) domain of TEL fused to the kinase domain of Syk. Expression of this fusion protein confers growth factor independence on Ba/F3

cells, while its expression in primary pre-B cells leads to lymphoid leukemia in mice (Kuno et al., 2001; Wossning et al., 2006). In Ba/F3 cells, expression of TEL-Syk leads to the activation of numerous signaling pathways, including the PI3 kinase/AKT and MAP kinase pathways, as well as activation of cytokine signaling pathways downstream of JAK2 (through phosphorylation of STAT5) (Kanie et al., 2004). In pre-B cells, TEL-Syk expression leads to a general increase in tyrosine phosphorylation, though specific pathways were not defined (Wossning et al., 2006).

Initial studies demonstrated that TEL-Syk-mediated transformation is dependent on oligomerization of the PNT domain of TEL, while more recent studies demonstrated that the Syk kinase domain is equally important (Kuno et al., 2001; Wossning et al., 2006). Yet, the question still remains whether expression of TEL-Syk in mouse hematopoietic stem cells will induce a myeloid malignancy resembling the human disease from which the fusion protein was identified. To address this question, we retrovirally transduced TEL-Syk into mouse fetal liver cells and then studied the growth of these cells in culture or following adoptive transfer into irradiated recipient mice. TEL-Syk expression in fetal liver hematopoietic cells led to an aggressive form of myelodysplasia accompanied by fibrosis that was dependent on the kinase domain of Syk and independently induced STAT5 phosphorylation despite JAK2 inhibition.

3.2 RESULTS

3.2.1 TEL-Syk is a hyperactive kinase that induces increased proliferative responses in hematopoietic progenitors.

Previous studies have demonstrated that expression of TEL-Syk in Ba/F3 cells leads to growth factor-independent proliferation and deregulated signal transduction (Kanie et al.,

2004; Kuno et al., 2001). We compared the biochemical activity of TEL-Syk and Syk by expression in HEK 293T cells. TEL-Syk was much more active in an *in vitro* kinase assay and heavily phosphorylated the downstream target NTAL compared to Syk (Fig. 3.1, A and B). We further wanted to determine if autophosphorylation was dependent on the kinase domain; thus, we engineered a kinase inactive version. A K473A replacement rendered TEL-Syk catalytically inactive. As expected, TEL-Syk KD failed to autophosphorylate and phosphorylate NTAL.

To investigate the biological activity of Syk, TEL-Syk and TEL-Syk KD in vivo we introduced these genes into BALB/c fetal liver hematopoietic cells by retroviral infection. Using a retroviral vector containing an IRES-GFP reporter, we were able to follow the efficiency of viral transduction by flow cytometry. Transduction efficiency of fetal liver hematopoietic cells varied from an average of 10% GFP with vector only infected cells to less than 5% GFP of cells with Syk, TEL-Syk or TEL-Syk KD viruses (data not shown). For *ex vivo* analysis we sorted transduced cells by flow cytometry, then assessed their growth potential at various cytokine concentrations by CFU assays in methylcellulose. A cocktail of SCF, IL-6, and IL-3 supported myeloid progenitor colony formation in cells expressing the retroviral vector alone, Syk or TEL-Syk KD at 1X stimulation. Ten-fold serial dilutions of the cytokine cocktail did not affect TEL-Syk colony formation, but did lead to loss of colony formation and cell expansion in the controls (Fig. 3.1, C and D). At 1X stimulation, TEL-Syk transduced fetal liver hematopoietic cells produced similar numbers of colonies, but the colony sizes were much larger and there was ~5 fold increase in the number of cells extracted from the methylcellulose medium (Fig. 3.1 D). In the complete absence of any cytokines, no

colonies were observed in any retrovirally-transduced cells. TEL-Syk expressing cells also showed increased proliferative responses to GM-CSF alone in CFU assays (data not shown). These data demonstrate that expression of TEL-Syk in fetal liver hematopoietic cells results in hypersensitivity to cytokines.

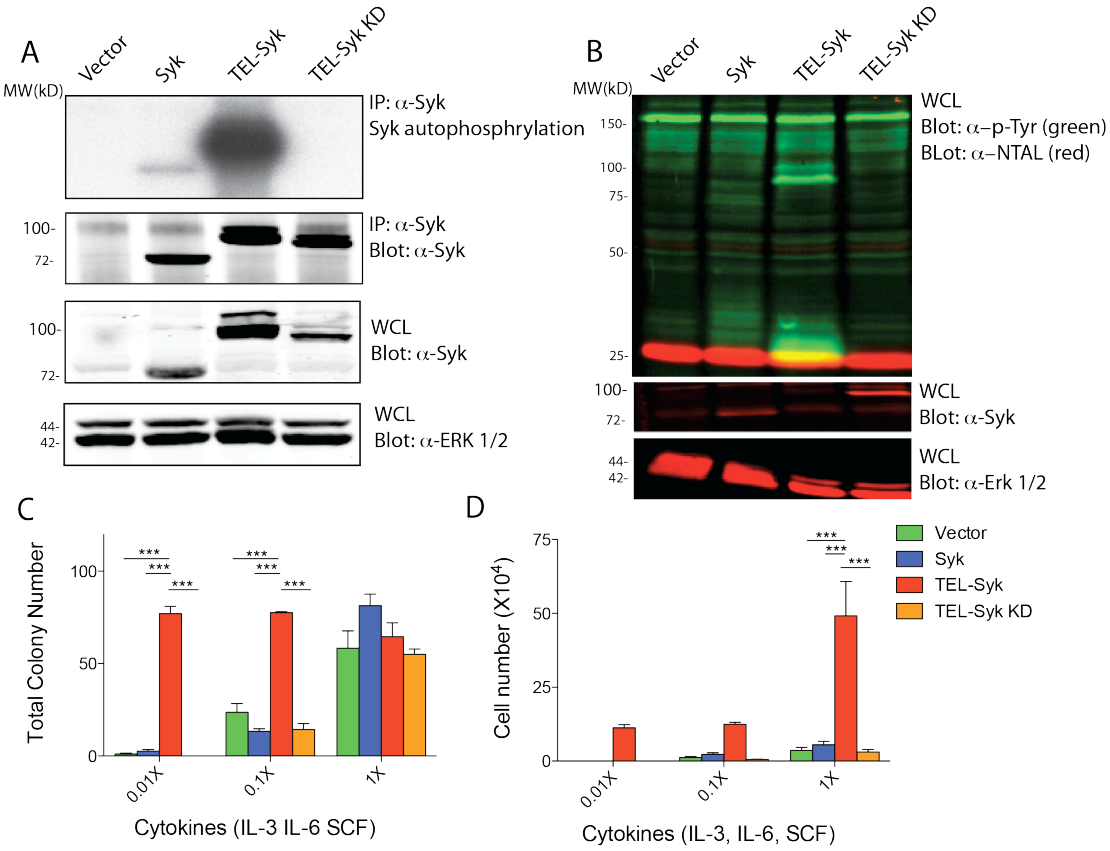

Figure 3. 1 TEL-Syk is constitutively active and confers hypersensitivity to low cytokine levels. (A) Autophosphorylation of TEL-Syk. HEK293T cells were transiently transfected with empty vector, Syk, TEL-Syk, and TEL-Syk KD. For the *in vitro* kinase assay, cell lysates were immunoprecipitated with anti-Syk then incubated with P^{32} labeled ATP. Immunoblots showing levels of Syk, TEL-Syk and TEL-Syk KD are shown below. The level of ERK1/2 was used as a loading control. (B) Phosphorylation of NTAL and other cellular proteins by TEL-Syk. HEK293T cells were transiently co-transfected with NTAL plus empty vector, Syk, TEL-Syk, or TEL-Syk KD. Whole cell lysates immunoblotted as indicated (C-D) Expression of TEL-Syk leads to growth factor hypersensitivity in fetal liver hematopoietic progenitors. BALB/c fetal livers were transduced with a retrovirus carrying empty vector, Syk, TEL-Syk, or TEL-Syk KD, sorted based on GFP expression, and plated in methylcellulose at a range of cytokine concentrations. Total numbers of colonies (C) and total cell numbers (D) were determined 12 days after plating. Experiments were conducted in triplicate and data is expressed as ± SEM. Statistical significance was determined by one-way ANOVA. *P< 0.05, **P< 0.01, ***P< 0.001. Data is representative of 2 independent experiments

3.2.2 Adoptive transfer of TEL-Syk expressing hematopoietic progenitors leads to myeloid cell expansion and mortality.

To examine the consequences of TEL-Syk expression in fetal liver hematopoietic cells *in vivo*, we adoptively transferred retrovirally transduced cells into irradiated recipient mice. As shown in Fig. 3.2 A, mice receiving TEL-Syk-transduced fetal liver cells had a significantly greater mortality rate post-transfer than animals receiving Syk- or TEL-Syk KD-transduced cells, with the majority of the mice dying within 60 days after cell transfer.

CBC analysis of peripheral blood following cell transfer demonstrated an increase in leukocytes at day 30 (Fig. 3.2 B), which were primarily myeloid-derived, in mice receiving TEL-Syk transduced fetal liver hematopoietic cells (Fig 3.2, C-E). At 30 days post-transfer, neutrophils and eosinophils were also significantly increased compared to controls, while monocytes were modestly increased. Lymphocyte numbers (Fig. 3.2 F) remained at consistent levels between TEL-Syk and the controls over 60 days. Robust neutrophil and eosinophil cell numbers in TEL-Syk chimeras correlated with disease severity, since the elevated myeloid cells at 30 and 45 days coincided with death of diseased mice. These data strongly suggests that myelo-expansion plays a role in TEL-Syk chimeric morbidity and mortality.

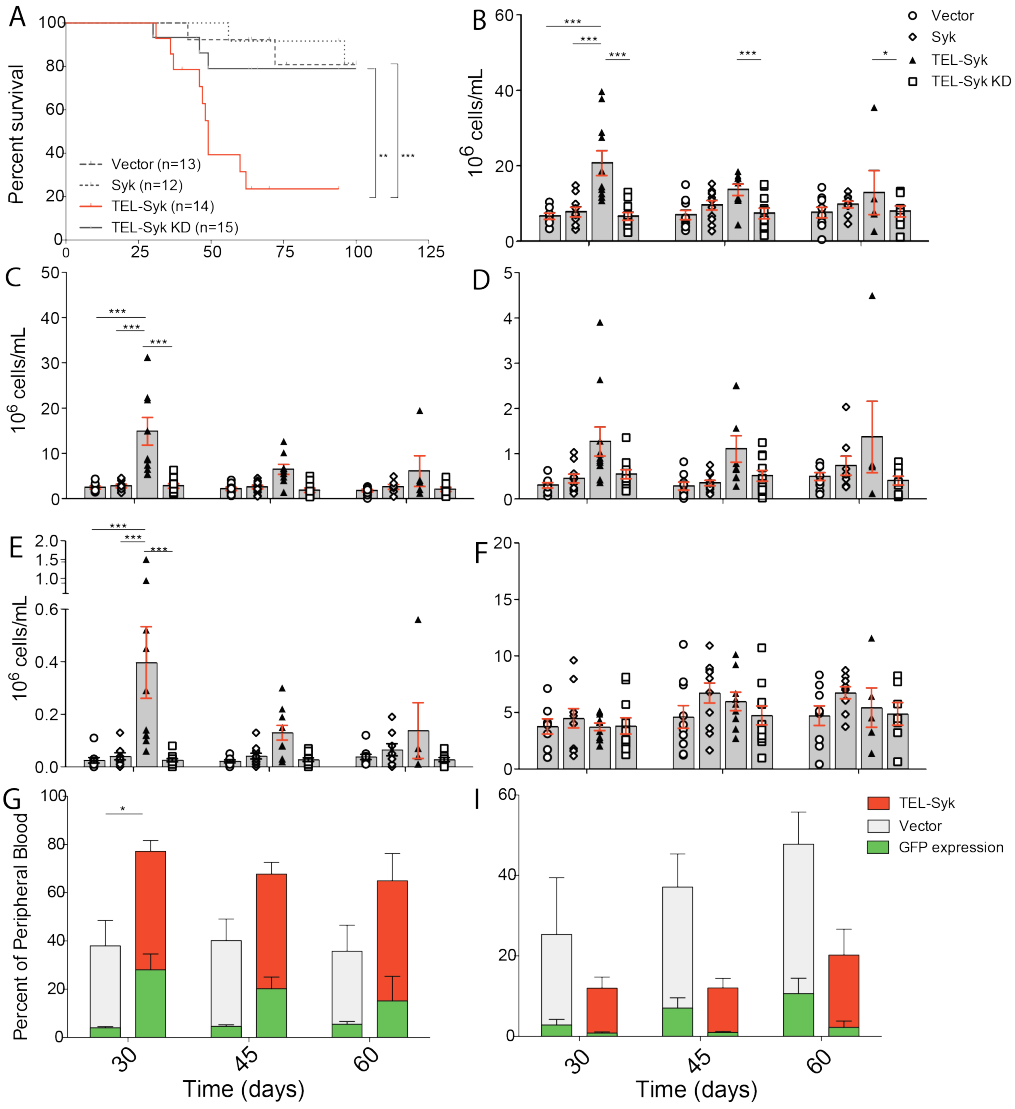

Figure 3. 2 TEL-Syk induces death *in vivo* and leads to myeloid cell expansion. (A) Kaplan-Meier survival curve of BALB/c recipients injected with fetal liver cells infected with retroviruses containing empty vector, Syk, TEL-Syk, or TEL-Syk KD. BALB/c fetal liver cells were spin-infected with retroviral supernatants containing the indicated viruses, then cultured for 2 days ex vivo, after which 5 x 106 cells of these cells were transferred into 2-3 month old lethally irradiated recipients. Survival was followed after successful hematopoietic reconstitution. Survival data is shown for vector (n=13), Syk (n12), TEL-Syk (n=14), and TEL-Syk KD (n=15) recipients. (B-F) CBC analysis of peripheral blood collected at the indicated days after transfer, showing total white blood cell levels (B), neutrophils (C), monocytes (D), eosinophils (E), and lymphocytes (F). Each data point indicates a single animal. Data are shown as mean ± SEM for vector (n=10), Syk (n=11), TEL-Syk KD (n=10), TEL-Syk (n=10). (G) At indicated time points, peripheral blood was isolated and stained for CD11b, Ly6G and CD19 then analyzed by flow cytometry. Plots show the total percentage of CD11b+Ly6G+ neutrophils (G) or CD19+ B cells (H), with green bars indicating the percentage of cells expressing GFP within these subsets, indicating that they were retrovirally transduced. Data are shown as mean ± SEM for vector (n=10) or TEL-Syk (n=10) expressing mice. Statistical significance was determined by one-way ANOVA. *P< 0.05, **P< 0.01, ***P< 0.001. For TEL-Syk, 8 mice survived to day 45 and 4 mice survived to day 60

We performed flow cytometry on peripheral blood samples from adoptively transferred mice, (Fig. 3.3). We found that neutrophils, defined as $Ly6G^{+}CDllb^{+}$ cells, were elevated at all time points, but most dramatically at 30 days post transfer, just before significant numbers of mice began to die, while numbers of B and T cells were not significantly different from control mice. Staining with anti-CD11b and anti-Siglec-F antibodies confirmed the dramatic eosinophilia in mice receiving TEL-Syk-expressing fetal liver hematopoietic cells (Fig. 3.3 E). In contrast, mice receiving Syk or TEL-Syk KD-transduced fetal liver hematopoietic cells showed no significant hematopoietic abnormalities compared to vector alone.

Examination of peripheral blood cells for expression of the linked GFP marker in the retrovirus confirmed that expression of TEL-Syk in fetal liver hematopoietic cells affected only myeloid cell development and not B-lymphocytes. Despite the fact that less than 5% of fetal liver hematopoietic cells were transduced with TEL-Syk, by 30 days following transfer ~30% of myeloid derived cells were GFP^{+} while the percentage of GFP^{+} B-lymphocytes remained low (Fig. 3.3 G). RT-PCR analysis confirmed that TEL-Syk was only expressed in GFP+ cells, and these cells also showed increased levels of phosphotyrosine (Fig. 3.4 A and B). These data indicate that expression of TEL-Syk in fetal liver cells drives a cell intrinsic expansion of myeloid lineage cells.

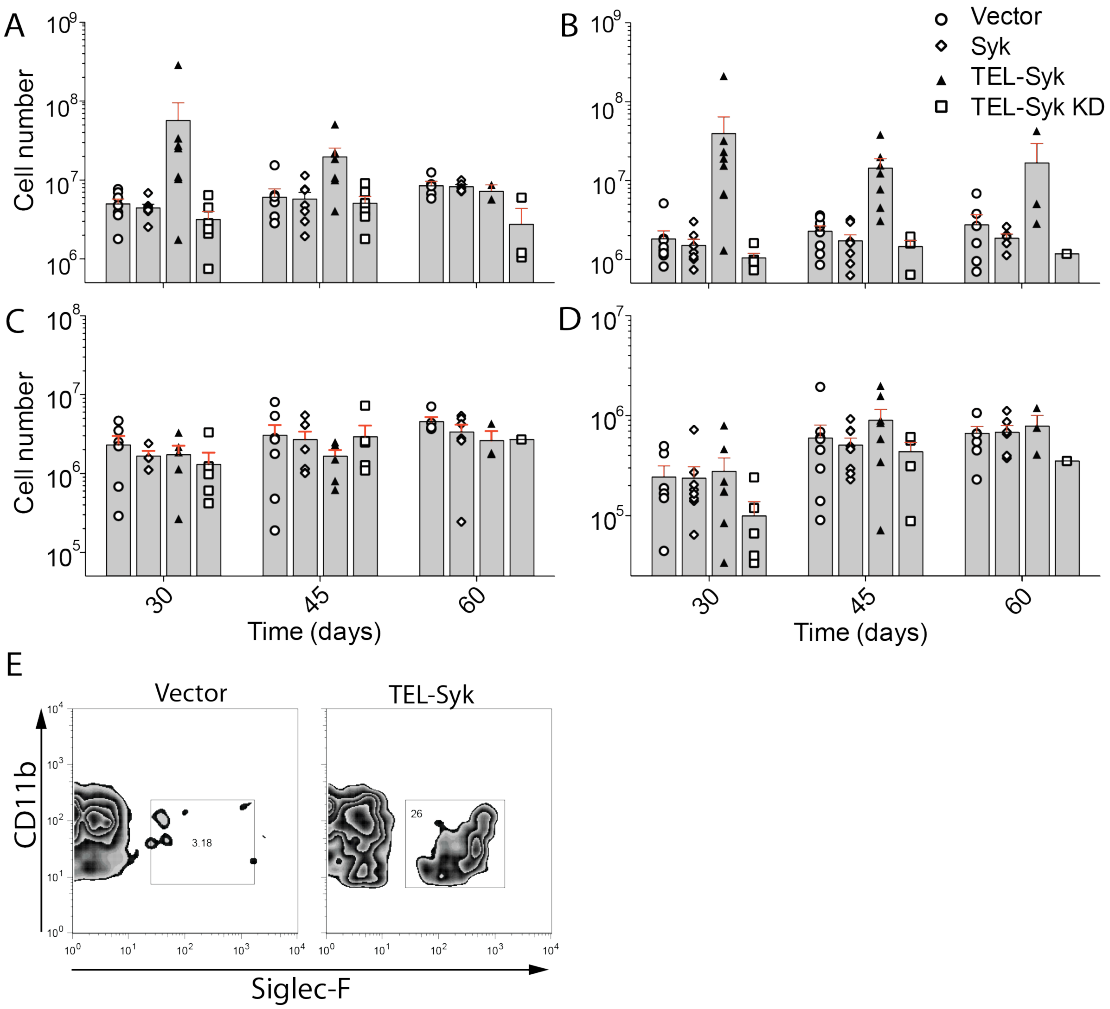

Figure 3. 3 TEL-Syk leads to myeloid cell expansion. Analysis of peripheral blood by flow cytometry. (A) Total cell numbers, and (B) neutrophils (Ly6G+ CD11b+), (C) B-cells (CD19+), (D) T-cells (TCRb+) and (E) Siglec-F expression was analyzed on Ly6G- peripheral blood from vector and TEL-Syk mice at 30 days.

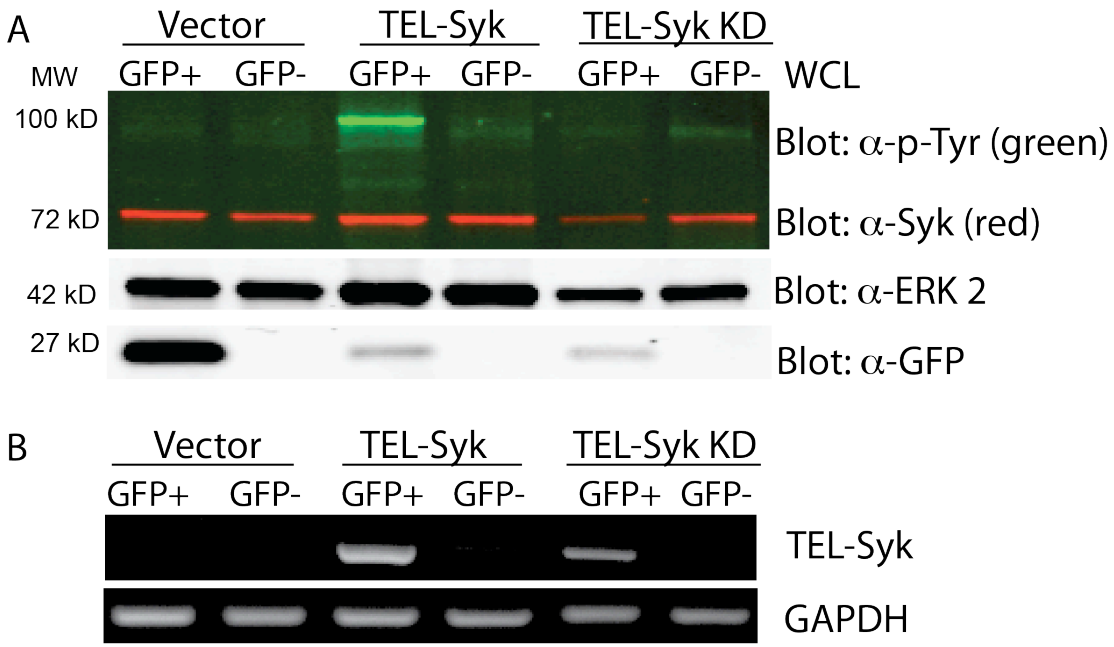

Figure 3. 4 Presence of GFP confirms TEL-Syk expression in bone marrow cells. (A) Immunoblots of $5x10^5$ sorted GFP^+ and GFP^- bone marrow cells from TEL-Syk and control mice stained with indicated antibodies (C) Detection of TEL-Syk transcripts by RT-PCR from $1x10^5$ sorted GFP^+ and GFP^- bone marrow cells from TEL-Syk and control mice. The level of GAPDH was used as a control.

3.2.3 TEL-Syk induces anemia and erythrodysplasia

Aside from myeloid cell expansion, another hallmark feature of MDS is erythrodysplasia. Indeed, mice transplanted with TEL-Syk transduced fetal liver hematopoietic cells showed erythroid cell abnormalities compared to mice receiving vector, Syk or TEL-Syk KD transduced cells. Erythrocyte number and total hemoglobin levels progressively decreased in mice receiving TEL-Syk transduced cells (Fig 3.5, A and B), while the remaining cells showed dysplastic features as measured by increased volume (MCV) and size (RDW) (Fig 3.5, C and D). Erythrodysplasia was readily apparent in blood smears from mice receiving TEL-Syk transduced fetal liver hematopoietic cells, as evidenced by extensive poikilocytosis and the presence of stomatocytes, dacrocytes, acanthocytes, and spheroctyes (Fig. 3.5 E).

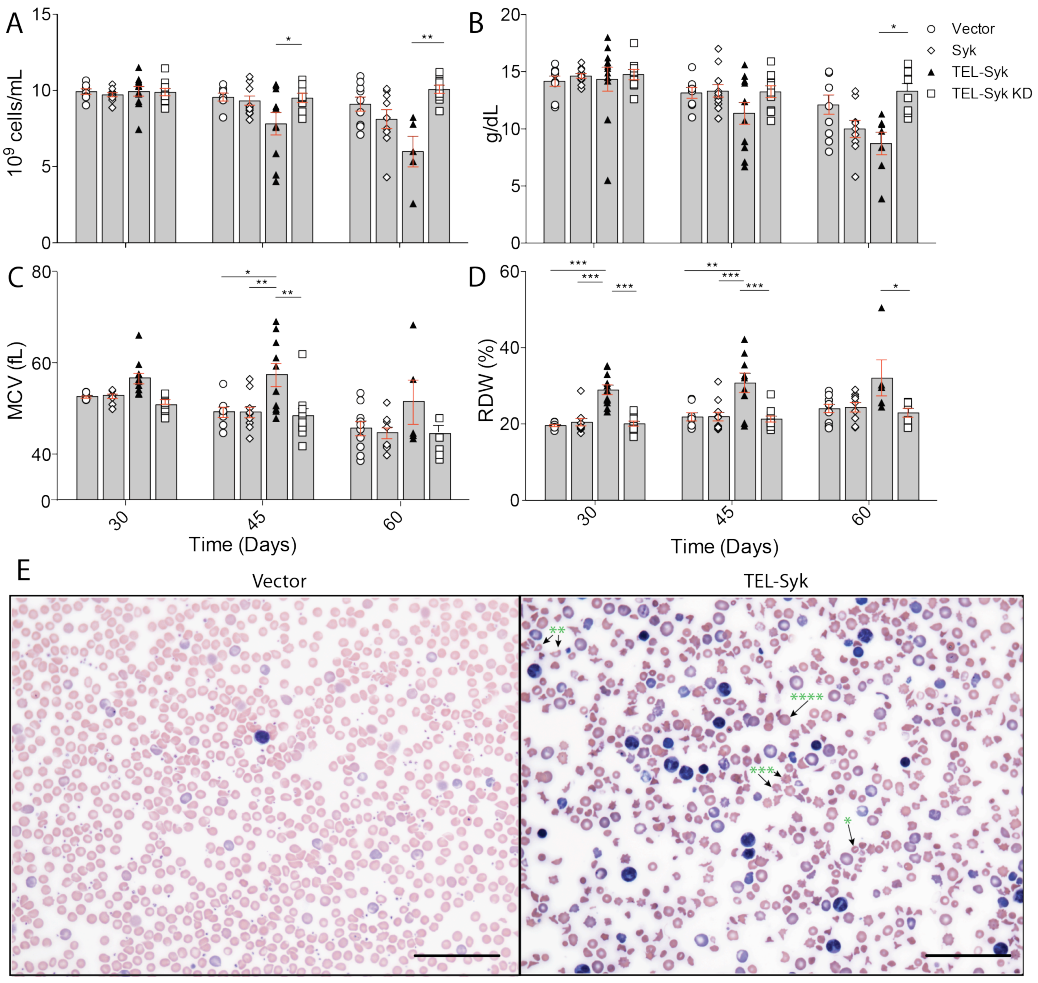

Figure 3. 5 TEL-Syk induces dyserythropoiesis *in vivo*. (A-C) Peripheral blood from BALB/c recipients injected with fetal liver cells transduced with the indicated retroviruses was collected at the indicated days after transfer and assessed by CBC analysis for (A) red blood cell counts, (B) hemoglobin levels, (C) mean corpuscular volume, (D) red cell distribution width. (E) Wright-Giemsa stains of peripheral blood smears from 45 days post-reconstituted TEL-Syk and vector mice. Stomatocytes, dacrocytes, acanthocytes, and spheroctyes are indicated in *, **, ***, ****. Scale bars correspond to 100 µm. Data are shown as mean ± SEM for vector (n=10), Syk (n=11), TEL-Syk KD (n=10), TEL-Syk (n=10) and statistical significance was determined by one-way ANOVA. *P< 0.05, **P< 0.01, ***P< 0.001.

3.2.4 Adoptive transfer of TEL-Syk expressing fetal liver hematopoietic cells leads to hypocellular splenomegaly, and extramedullary hematopoiesis in the liver.

To evaluate the effects of TEL-Syk expression in progenitors in secondary lymphoid organs, we examined the spleens of mice at 60 days post transfer. TEL-Syk expressing mice showed splenomegaly (Fig. 3.6, A and B). Surprisingly, however, this splenomegaly was not due to increased cell numbers and in fact the TEL-Syk expressing

mice had approximately 2 fold fewer cells in total, resulting in nearly a 5 fold difference in the ratio of cell number to mg of spleen (Fig. 3.6, C and D). The cells in the spleens of the TEL-Syk expressing mice were mainly $Ly6G^+CD11b^+$ neutrophils or $F4/80^+CD11b^+$ monocytes/macrophages, with a lower percentage of T- and B-lymphocytes, compared to the spleens of vector, Syk or TEL-Syk KD expressing mice (Fig. 3.6 E). The remaining unidentified cell types are likely infiltrating eosinophils and dysplastic erythrocytes. The histology of spleens from TEL-Syk expressing mice revealed disrupted follicular structures, a paucity of red pulp, islands of erythroid bodies, and large patches of connective tissue (Fig. 3.6 G). At higher magnification, the spleens of TEL-Syk animals revealed apoptotic bodies, dysmyelopoiesis, aggregates of erythroid bodies, and eosinophilic infiltrates (Fig. 3.7, B-D). Cytospins of splenocytes demonstrated an increase in dysplastic neutrophils and abnormal monocytes with large disrupted nuclei in the TEL-Syk compared to vector expressing mice (Fig. 3.6, H and I). TEL-Syk expressing spleens showed dramatic increase in apoptosis compared to vector by immunohistochemical stains for activated caspase 3 mice (Fig. 3.6, J and K). To examine the causes of the hypocellular splenomegaly we looked for evidence of myelofibrosis in these tissues. Using Masson's Trichome staining, which stains collagen deposition, we found extensive fibrosis in both spleen (Fig. 3.6, L and M) and liver (Fig. 3.8, C and D) sections from mice receiving TEL-Syk transduced progenitors, but little collagen deposition in vector expressing mice. Finally, the livers of the mice receiving TEL-Syk transduced fetal liver hematopoietic cells showed extensive hematopoietic cell infiltration and connective tissue accumulation (Fig. 3.8, A and B). Thus, despite the myeloid cell expansion in the peripheral blood caused by TEL-Syk expression, the spleens from these

animals develop progressive hypocellularity and fibrosis associated with high levels of cell death.

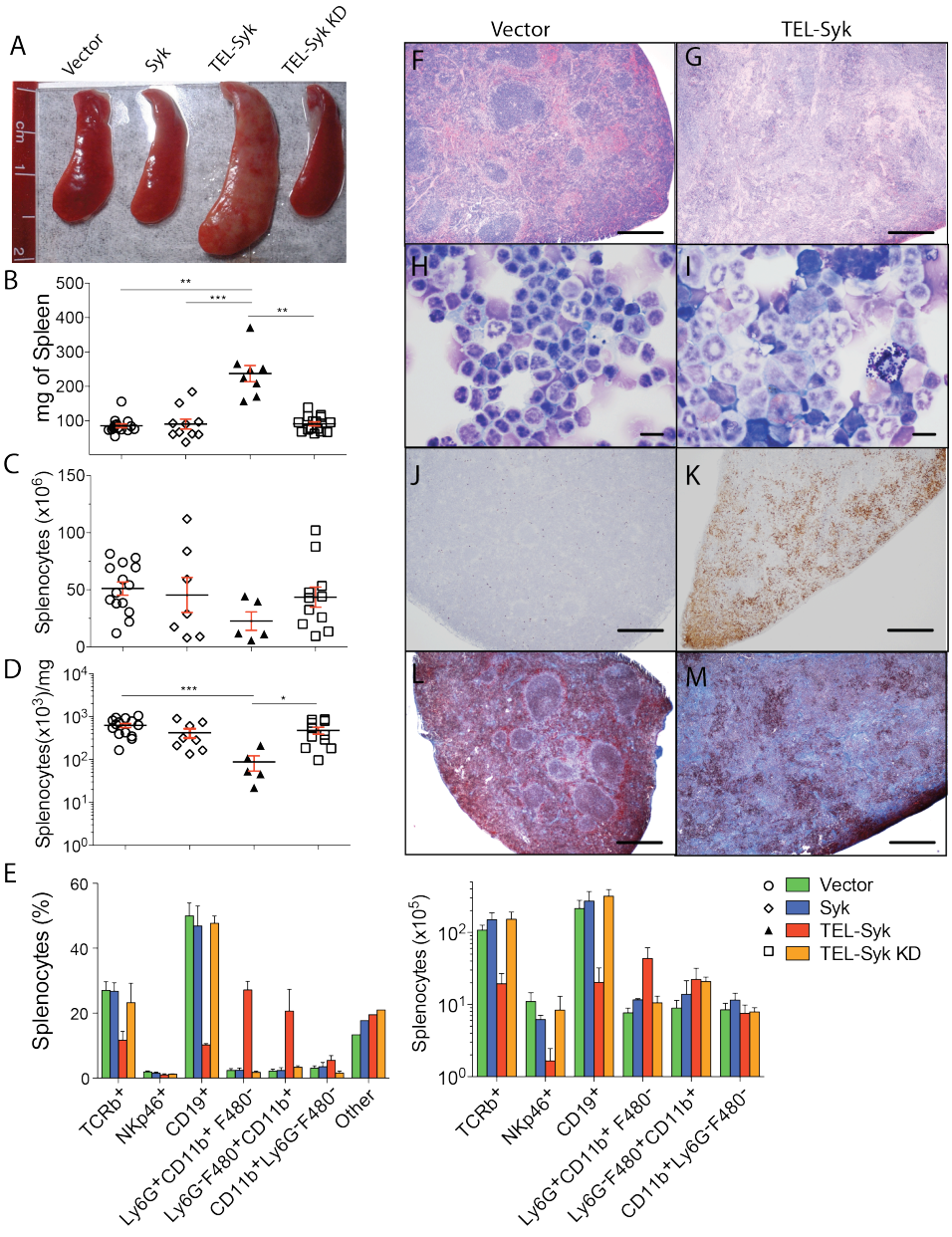

Figure 3. 6 TEL-Syk expression leads to splenomegaly, with hypocellularity and apoptosis. (A) Spleens from vector, Syk TEL-Syk and TEL-Syk KD expressing mice that were sacrificed at 60 days post cell transfer. (B) Splenic weights, (C) the ratio of splenocytes per mg of spleen, and (D) Total numbers of splenocytes from chimeric mice. (E) Flow cytometric analysis of splenic leukocytes. Data are shown as mean ± SEM for vector (n=4), Syk (n=3), TEL-Syk (n=4), TEL-Syk KD (n=4). (F, G) H&E stained sections of spleens from vector and TEL-Syk expressing mice. (H, I) Wright-Giemsa stained cytospins of splenocytes from TEL-Syk and vector chimeras. (J, K) Spleen sections from vector and TEL-Syk expressing mice stained with anti-cleaved capase-3 antibodies (L, M) Masson's Trichrome stained sections of spleens from vector and TEL-Syk chimeras. Scale bars correspond to (F, G, K-M) 500 µm, and (H, I) 10 µm respectively. Statistical significance was determined by one-way ANOVA. *P< 0.05, **P< 0.01, ***P< 0.001.

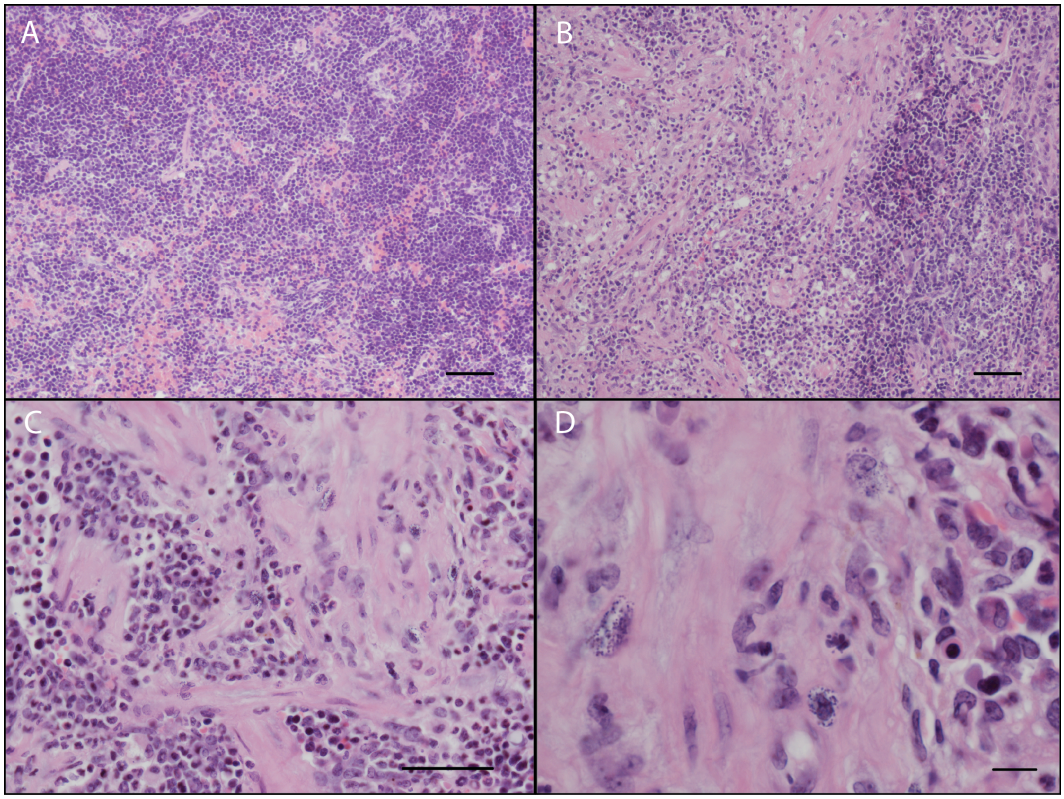

Figure 3. 7 TEL-Syk disrupts splenic architecture and induces dysplasia. H&E stained sections of spleens from (A) vector and (B-D) TEL-Syk expressing mice. Scale bars correspond to (A-C) 50 mm, and (D) 10 mm.

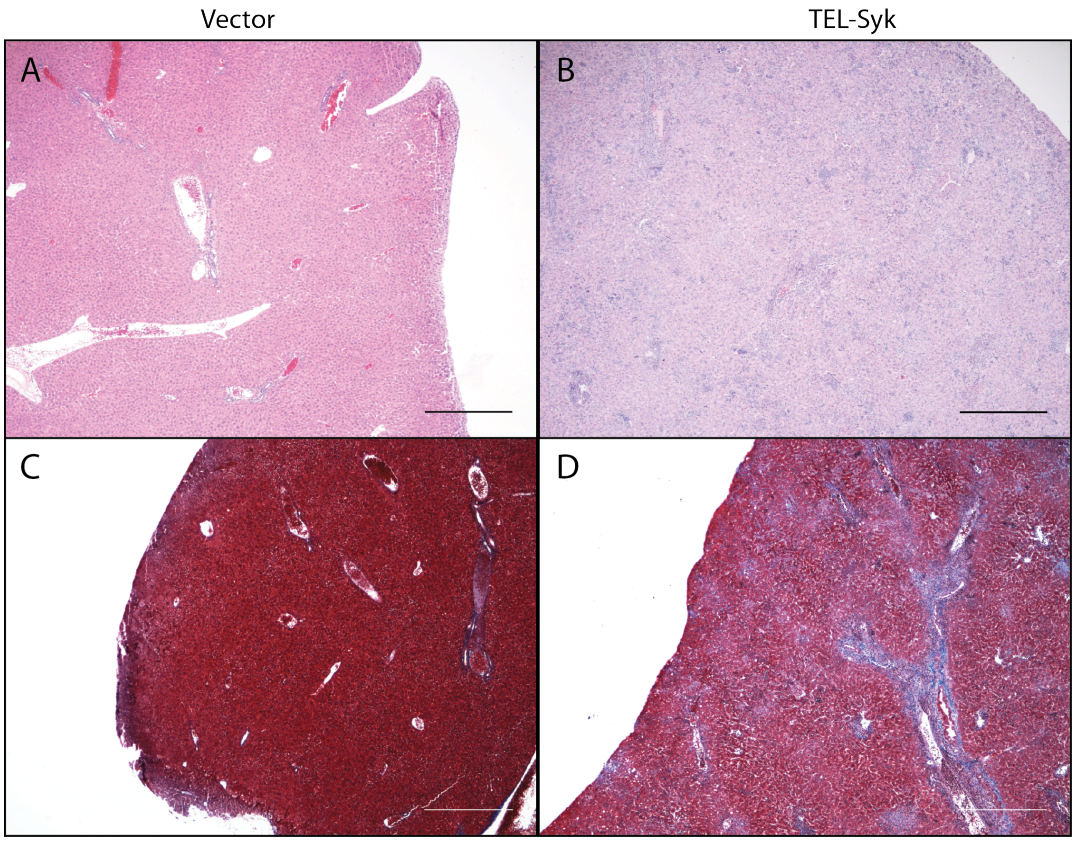

Figure 3. 8 TEL-Syk expression induces cellular infiltration in the liver. H&E staining of hepatic sections from (A) vector and (B) TEL-Syk expressing mice. Masson Trichrome's stain of hepatic sections from (C) vector and (D) TEL-Syk expressing mice. Scale bars correspond to (A-D) 500 μm.

3.2.5 Adoptive transfer of TEL-Syk expressing progenitors causes bone marrow failure

To examine the potential cause for the progressive decrease in peripheral white blood cells in mice receiving TEL-Syk transduced fetal liver cells, we examined the bone marrow of animals 60 days post cell transfer. Similar to the spleen, TEL-Syk expressing bone marrow demonstrated hypocellularity compared to control mice (Fig. 3.9 A). Myeloid cells were the predominant cell type in terms of percentages and numbers, with a relative loss of lymphoid cells in the TEL-Syk expressing mice, as determined by flow cytometry (Fig. 3.9 B). The bone marrow of TEL-Syk expressing mice showed extensive hypocellularity, abnormal hematopoiesis due to the absence of mature and immature

hematopoietic cells, and a large number of apoptotic bodies compared to animals receiving vector-transduced fetal liver hematopoietic cells (Fig. 3.9 C). This finding is further confirmed by bone marrow smears (Fig. 3.9 D) in which a general loss in cellularity and diversity of hematopoietic cells was observed. Bone marrow dysplasia was exemplified by the presence of mummified megakaryocytes (arrow) and dysplastic neutrophils (red asterisk) in the TEL-Syk expressing bone marrow (Fig. 3.9 I). We also found extensive fibrosis in sternum sections of TEL-Syk expressing mice, as determined by reticulin staining of histologic sections (Fig. 3.9, J and K). The reticulin staining corresponded to hypocellular bone marrow patches seen in H&E stained sections.

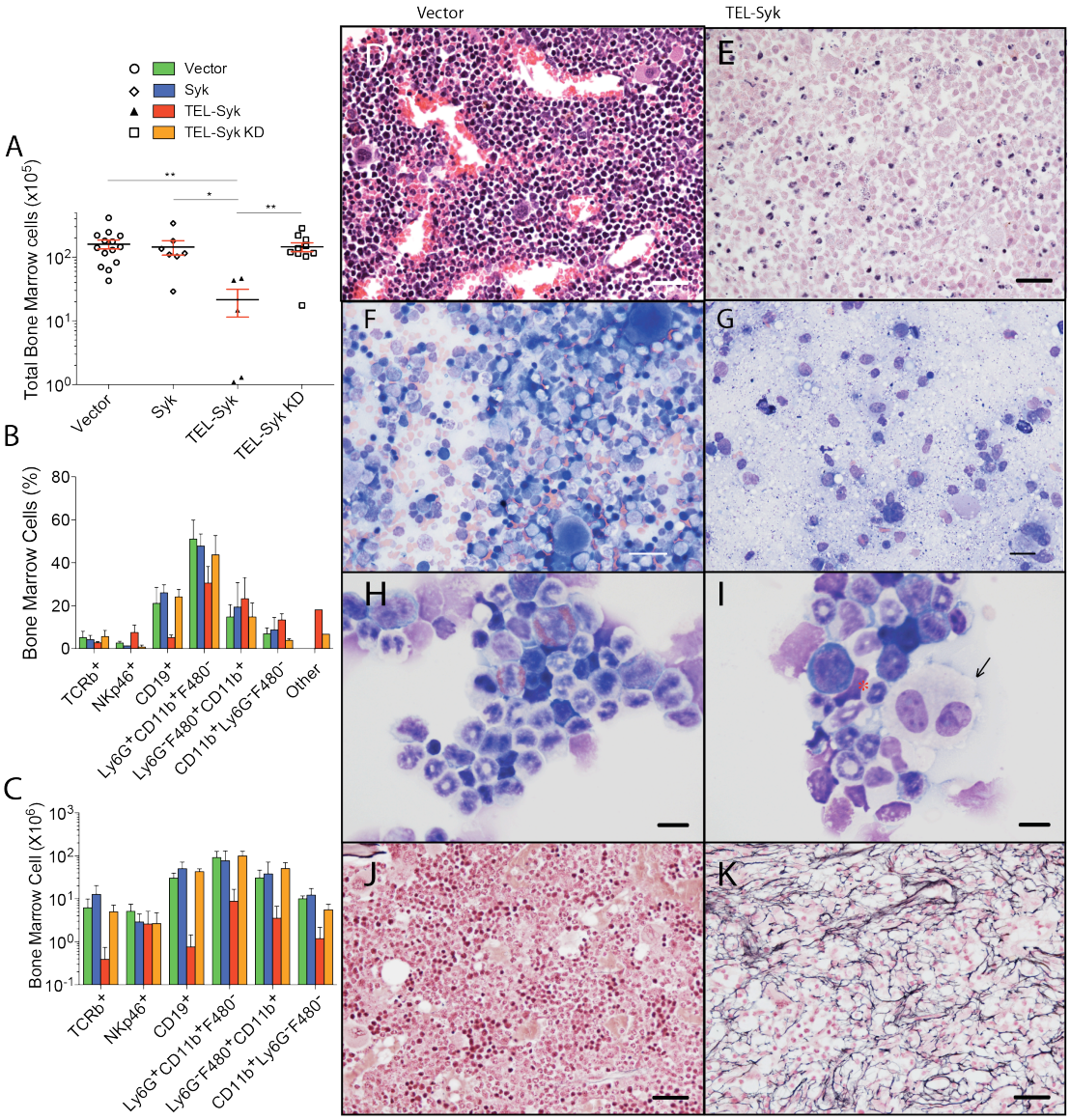

Figure 3. 9 TEL-Syk expression leads to bone marrow hypocellularity and dysplasia. (A) Numbers of bone marrow cells isolated from mice receiving vector, Syk, TEL-Syk KD and TEL-Syk transduced fetal liver hematopoietic cells. Flow cytometric analysis of (B) leukocytes percentages and (C) total leukocyte numbers in the bone marrow cells. (D, E) H&E stained sternum sections from vector and TEL-Syk expressing mice, (F, G) Wright-Giemsa staining of bone marrow smears, and (H, I) cytospins of bone marrow cells isolated from femurs and tibias of TEL-Syk and vector expressing mice at 60 days following cell transfer. Dysplastic megakaryocytes (arrow) and neutrophils (asterisk) are indicated. (J, K) Reticulin stained sternum sections from vector and TEL-Syk expressing mice. Scale bars correspond to (D-G, J, K) 30 µm, and (H, I) 10 µm. Data is shown as mean ± SEM for vector (n=4), Syk (n=3), TEL-Syk (n=4), TEL-Syk KD (n=4) and statistical significance was determined by one-way ANOVA. *P< 0.05, **P< 0.01, ***P< 0.001.

3.2.6 Mice receiving TEL-Syk transduced fetal liver hematopoietic cells had elevated levels of circulating inflammatory cytokines

To test the hypothesis that circulating growth factors could be driving the myeloid expansion in TEL-Syk expressing mice, we used an immunoblot array to measure serum cytokines from TEL-Syk and vector chimeras. As shown in Fig. 3.10 A, TEL-Syk expressing mice manifested elevated levels of a number of inflammatory cytokines, growth factors, chemokines and proteases, both at 45 and 60 days following fetal liver cell transfer. IL-12, IL-13, IFN-γ, MIG, and TCA-3 were robustly elevated at 30 days, while IL-6, G-CSF, IP-10, MCP-1, MIP-1α, TIMP-1 and TREM-1 became elevated at 60 days. To look for factors that may be particularly associated with fibrosis, we used an angiogenic array designed to examine a broader range of factors, assessing sera only from mice at 30 days following TEL-Syk transduction. On this array, the sera from TEL-Syk expressing mice showed increased levels of additional chemokines, (CXCL4, CXCL16), proteases (MMP3, 8, 9), protease inhibitors (TIMP-1) and binding proteins (IGFBP1, 2, 3, 9) (Fig. 3.10 B).

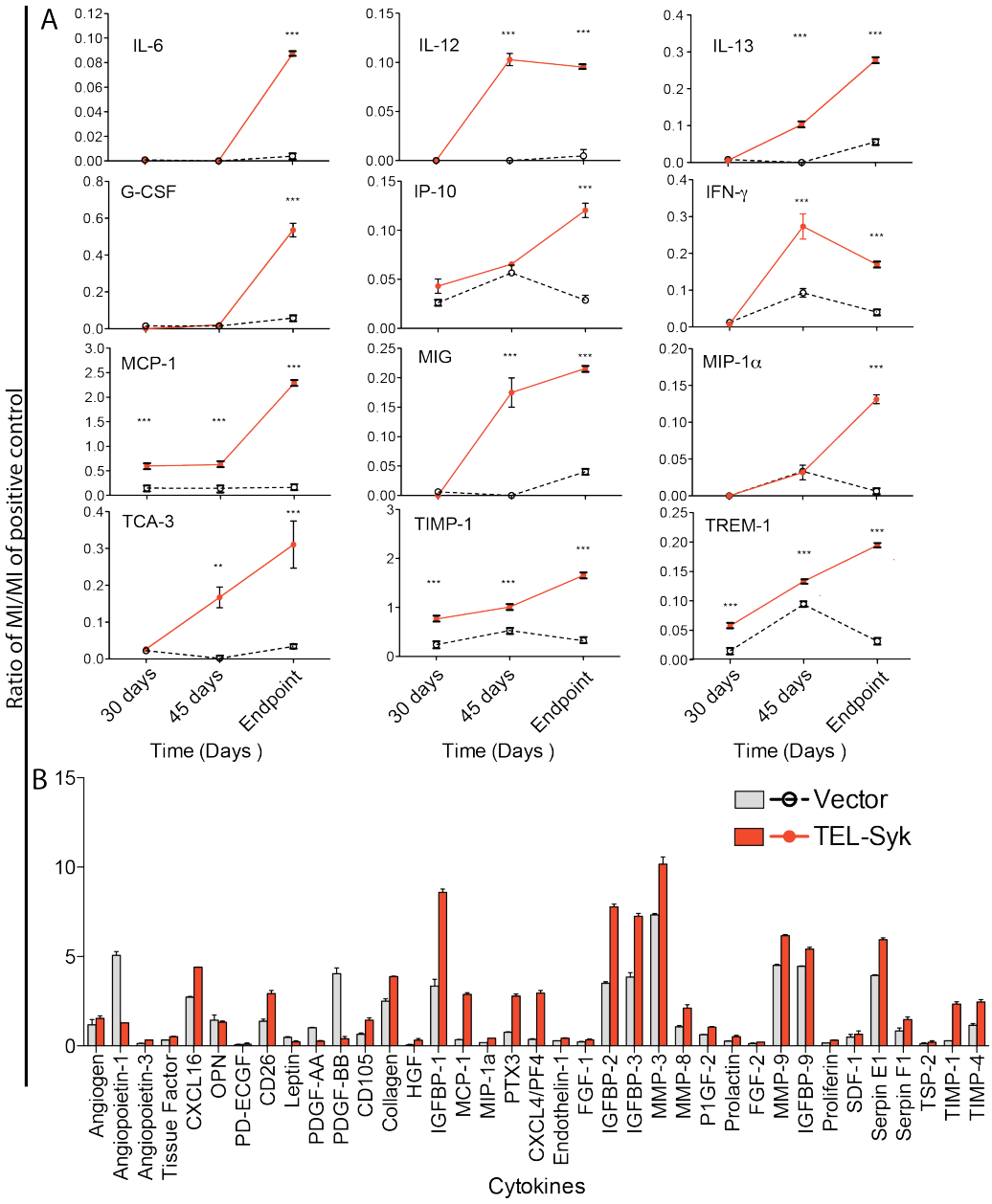

Figure 3. 10 TEL-Syk expression leads temporal increase in circulating inflammatory cytokines. (A) Pooled sera collected from TEL-Syk and vector expressing mice at 30 days, 45 days and endpoint, as determined by TEL-Syk morbidity, was examined using a Cytokine Profiler Array. Cytokine levels were represented as ratio of mean intensities of the given cytokine to a positive control after background intensity subtraction. (B) Representative histograms from 30-day old pooled sera collected from TEL-Syk and vector expressing mice using the Angiogenesis Array. Data are expressed as (A) means ± SEM (B) means ± SD. Statistical significance was determined by one-way ANOVA. *P< 0.05, **P< 0.01, ***P< 0.001.

3.2.7 TEL-Syk expressing cells show elevated levels of phospho-STAT5

To begin to assess the mechanism by which TEL-Syk expression in hematopoietic cells drives myeloid expansion, we examined overall tyrosine phosphorylation and levels of

phospho-STAT5 in cells from TEL-Syk expressing mice. Bone marrow cells from vector TEL-Syk, and TEL-Syk KD expressing animals, at 30 days following cell transfer, were sorted into GFP^+ versus GFP^- fractions and examined by immunoblot analysis. As shown in Fig. 3.3 A, the GFP^+ fraction of cells from TEL-Syk expressing mice showed higher levels of overall phosphotyrosine compared to GFP^- cells from mice receiving TEL-Syk transduced cells or both GFP^+ and GFP^- cells from vector expressing mice. A similar increase in total phosphotyrosine was also seen in TEL-Syk-retrovirally transduced fetal liver hematopoietic cells sorted for GFP^+ and GFP^- compared to vector, Syk and TEL-Syk KD (Fig. 3.11 A), To determine if STAT5 was phosphorylated in TEL-Syk expressing cells, we examined fetal liver for phospho-STAT5 by immunoblot analysis (Fig. 3.11 B) and intracellular staining (Fig. 3.11 C). The GFP+ TEL-Syk infected cells showed constitutive STAT5 phosphorylation compared to controls, which was apparent even in cells that were cytokine/growth factor starved for 6 hours prior to examination (Fig. 3.11 C, left panel). Restimulation with cytokines demonstrated an enhancement of phospho-STAT5 levels in fetal liver cells (Fig. 3.11, C and D).

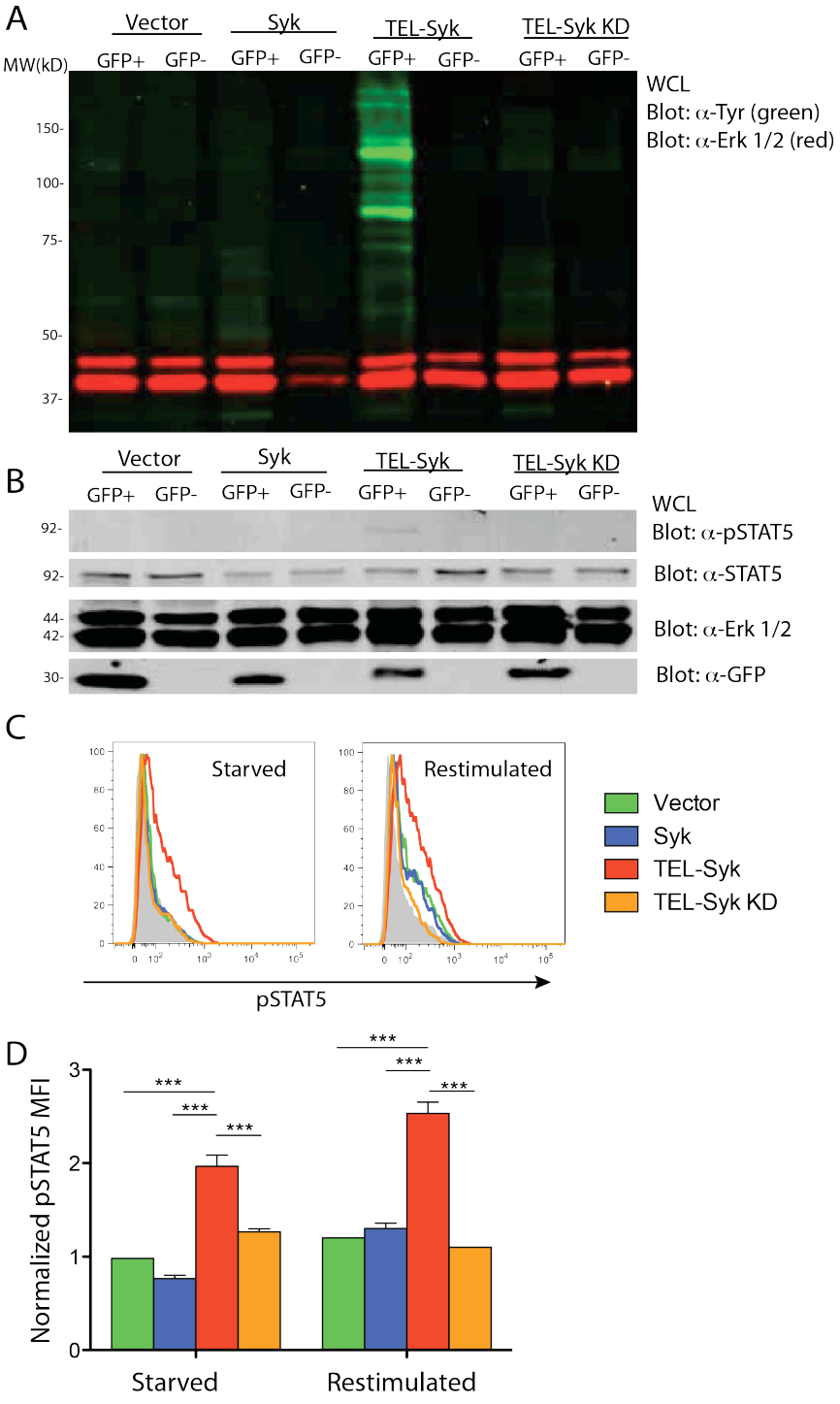

Figure 3. 11 Elevated STAT5 phosphorylation in fetal liver cells expressing TEL-Syk. (A and B) Lysates of sorted GFP$^+$ and GFP$^-$ fetal liver cells were analyzed by SDS-PAGE and imunoblotted with indicated antibodies. (C) Representative histograms of retrovirally transduced fetal liver cells starved for 6 hours, and restimulated with cytokines (IL-3, IL-6, SCF). Cells were fixed, permeabilized and levels of phospho-STAT5 in the GFP$^+$ cells was determined. (D) Normalized MFI of phospho-STAT5 in retrovirally transduced fetal liver cultured for 3 days in cytokines, followed by a 6 hour starvation and 30 minute restimulation. Phospho-STAT5 MFIs were normalized to starved vector expressing cells. Statistical significance was determined by one-way ANOVA. *P< 0.05, **P< 0.01, ***P< 0.001.

3.2.8 JAK inhibition fails to abolish TEL-Syk hypersensitivity and STAT5 phosphorylation

To determine whether the high level of phospho-STAT5 in TEL-Syk expressing cells was due to activation of the upstream kinase JAK2 or mediated via direct phosphorylation of STAT5 by TEL-Syk, we examined cytokine responses and STAT5 phosphorylation in response to cytokines in the presence or absence of a JAK2 inhibitor. For these experiments, we used GM-CSF stimulation, which signals through JAK2 to STAT5 to drive proliferation of hematopoietic cells. As shown in Fig. 3.12 A, we found that the JAK2 inhibitor reduced colony formation of fetal liver cells transduced with vector, Syk or TEL-Syk KD in a dose dependent manner compared to DMSO treated controls, while fetal liver hematopoietic cells transduced with TEL-Syk were resistant to JAK2 inhibition and demonstrated 55-75% of colony formation compared to vehicle control. At high levels of the JAK2 inhibitor vector, Syk and TEL-Syk KD failed to form colonies, while TEL-Syk drove colony formation. Using intracellular staining/flow cytometry, we found that TEL-Syk expressing fetal liver hematopoietic cells showed readily detectable levels of phospho-STAT5, in the absence of GM-CSF, which was not affected by increasing doses of the JAK2 inhibitor (Fig. 3.12 B). Stimulation of these cells with GM-CSF led to high levels of phospho-STAT5 in all cell types, but was highest in the TEL-Syk transduced cells. STAT5 phosphorylation was reduced to baseline by exposure to 5 μM JAK2 inhibitor in vector, Syk and TEL-Syk KD expressing cells, but was still present, at a level equivalent to unstimulated cells, in TEL-Syk transduced fetal liver hematopoietic cells (Fig. 3.12 B). These data indicate that TEL-Syk expression leads to constitutive STAT5 phosphorylation in resting cells, which is independent of JAK2, but very high levels of phospho-STAT5 in stimulated cells, which is mediated predominately through

JAK2. The deregulated signaling through STAT5 in TEL-Syk expressing progenitors likely contributes to the myeloproliferation and dysplasia found in TEL-Syk transduced mice.

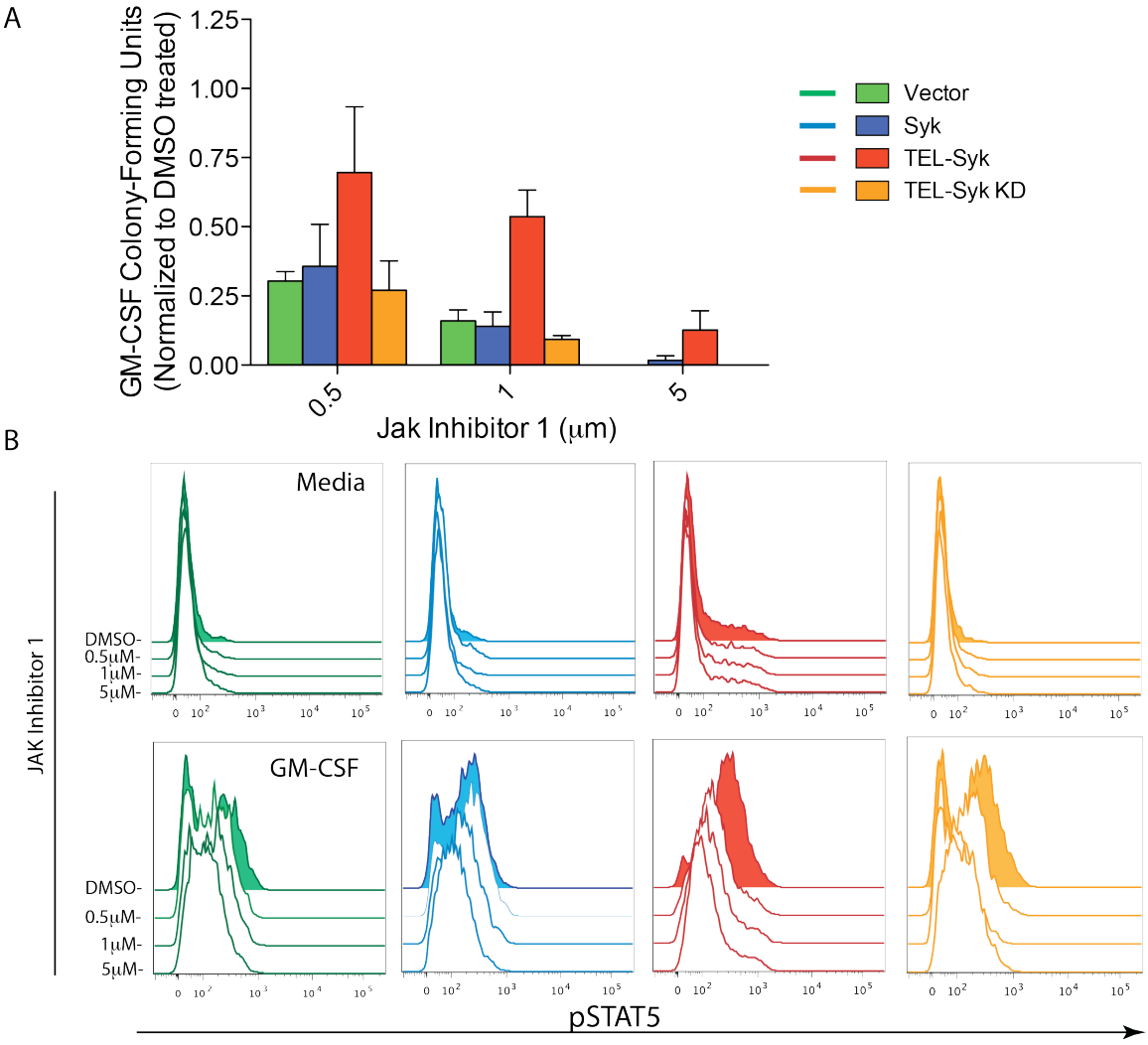

Figure 3. 12 TEL-Syk promotes colony formation and STAT5 phosphorylation independently of JAK2 activity. (A) JAK2 inhibition was determined by assessing colony formation of sorted GFP+ fetal liver cells in methylcellulose. Colony numbers were normalized against a DMSO control for each cell type and represented as a percent of maximal growth after 7 days in culture in 10 ng/mL GM-CSF. (B) Histograms show phospho-STAT5 levels in sorted GFP^{+} fetal liver cells starved for 6 hours and restimulated for 30 minutes with or without 50 ng/mL GM-CSF in the presence of the JAK inhibitor 1 at the indicated concentrations, measured by flow cytometry. Experiments were conducted in triplicate. Statistical significance was determined by one-way ANOVA. *P< 0.05, **P< 0.01, ***P< 0.001.

3.3 Discussion

In this study, we report that introduction of TEL-Syk into fetal liver hematopoietic cells leads to a rapidly progressive myelodysplasia with dramatic splenic and bone marrow fibrosis, culminating in bone marrow and splenic hypocellularity. The rapid expansion of myeloid cells includes all lineages (neutrophils, monocytes, and eosinophils) with a concomitant reduction in lymphocytes. In addition to extramedullary hematopoiesis and subsequent dysplasia, TEL-Syk expressing mice demonstrated robust hematopoietic cell apoptosis as shown by increased cleaved caspase-3 staining. TEL-Syk mice showed elevated inflammatory cytokines in serum with increases in MMPs, IGFBPs and other angiogenic-related factors. We further demonstrate that fetal liver hematopoietic cells expressing TEL-Syk manifest elevated levels of STAT5 phosphorylation, in both resting and cytokine stimulated cells, which was partially resistant to JAK2 inhibition.

Expression of TEL-Syk in fetal liver progenitor cells induces colony formation and proliferation at very low cytokine levels (which otherwise do not support normal progenitor proliferation) due to hyperactivation of cytokine signaling pathways such as JAK2/STAT5. Besides being hyperresponsive to proliferation inducing cytokines, we found that expression of TEL-Syk leads to over production of a number of proinflammatory cytokines. It is likely that cytokine overproduction establishes a paracrine feedback loop that drives myeloid cell proliferation and dysplasia in TEL-Syk expressing cells. An investigation of how TEL-Syk expands or attenuates progenitor populations -- specifically multipotent progenitor, common myeloid progenitors, granulocyte/macrophage progenitors, or megakaryocyte/erythrocyte -- would provide

further insight into abnormal hematopoiesis and subsequent leukemogenesis. Disruption of the hematopoietic progenitor populations was demonstrated in studies that examined the effect of BCR-ABL-induced myelodysplasia in mouse models (Reynaud et al., 2011). Expression of BCR-ABL in hematopoietic stem cells leads to a significant increase of splenic-derived myeloid progenitor populations, which contributes to myeloid cell expansion. In this model, overproduction of the proinflammatory cytokine IL-6 is crucial to maintain the myeloid cell expansion.

While expression of TEL-Syk in fetal liver hematopoietic cells induced rapid myeloproliferation with myleodysplasia, we did not observe outgrowth of blast-like cell types in these mice. Moreover, we were unsuccessful in adoptively transferring the myeloproliferative disease to secondary recipient mice, using either irradiated or non-irradiated hosts (data not shown). Therefore it is unlikely that the disease process we observed represented a myeloid cell malignancy, as is seen in mice receiving BCR-ABL transformed progenitor cells (Van Etten, 2002). It is likely that the very high apoptotic rate induced in myeloid cells by expression of TEL-Syk prevents establishment of myeloproliferation in secondary recipient mice.

When we introduced TEL-Syk into fetal liver hematopoietic cells, TEL-Syk leads to a myeloproliferative disease rather than lymphoid leukemia, which demonstrates a key difference between our data and experiments conducted by Wossning et al. (Wossning et al., 2006). In that work, the authors introduced TEL-Syk into differentiated pre-B cells, rather than a mixed population of hematopoietic cells, leading to $CD19^{+}$ lymphoid leukemia. The variability in disease phenotype is likely to be context dependent such that TEL-Syk introduced into a mixed population of hematopoietic cells yields a myeloid

disease, while TEL-Syk introduced into a lymphoid precursor yields a lymphoid leukemia. This effect has also been demonstrated in BCR-ABL^{+} CML (Reynaud et al., 2011), in which paracrine factors maintain lineage status, but the genetic lesion drives proliferation by deregulated signaling.

The extremely high rate of apoptosis we observed in TEL-Syk expressing mice is likely a major contributor to the bone marrow and splenic hypocellularity that developed in these animals. Increased hematopoietic cell apoptosis is a clinical characteristic of myelofibrosis associated with myeloproliferation in patients (Thiele and Kvasnicka, 2005). It is likely that the high rate of apoptosis limits the ability of fetal liver hematopoietic cells expressing TEL-Syk to develop secondary genetic changes which would lead to establishment of more long lived myeloproliferation or even leukemia. Indeed, chronic myeloproliferative diseases such as CML are associated with reduced rates of spontaneous apoptosis often through inhibition of stress responses (Yuan et al., 2011; Zhang et al., 2012).

Analysis of serum cytokines demonstrated an elevation of proinflammatory cytokines such as MCP-1, IL-13, MIP-1α, IL-6, IP-10, MIG, and TCA in mice receiving TEL-Syk expressing fetal liver hematopoietic cells. Increased proinflammatory cytokines have also been demonstrated in patients and in mouse models of primary myelofibrosis (Tefferi et al., 2011). Patients with primary myelofibrosis, with or without the presence of *JAK2V617F,* develop a proinflammatory cytokine signature that contains IL-6, MCP-1, MIG, MIP-1α, TNF-α and IP-10. The pathologic role of these cytokines is undetermined but their increase correlates with disease prognosis, in which elevation of IL-6, IL-2R, IL-1RA, MIP-1α, MIG, IL-8, IL-12, and IP-10 correlate with shortened primary

myelofibrosis survival. The authors of this study suggest that the initial myeloproliferation and the presence of inflammatory circulating cytokines are due to an abnormal bone marrow microenvironment propagated by pathogenic myeloid cells.

In our model, it is unclear which dysplastic myeloid cell lineage plays the dominant role in the development of fibrosis and elevation of circulating inflammatory cytokines in TEL-Syk mice. Basophils from patients with *JAK2V617F* polycythemia vera show an activated phenotype based on $CD63^{+}$ expression and an increase in the number of empty vesicles, presumably due to degranulation (Pieri et al., 2009). Activation of neutrophils in response to immune insults rapidly induces the release of pre-stored proinflammatory cytokines and proteases from a number of secretory vesicles (Nathan, 2006). In accordance with elevated circulating proinflammatory cytokines and MMPs seen in TEL-Syk serum, aberrant activation and degranulation of dysplastic myeloid cells could be a source for these circulating factors. In contrast, neutrophils from patients with MDS demonstrate a blunted response to proinflammatory cytokines such as IL-8 and GM-CSF, thereby contributing to poor bactericidal responses (Fuhler et al., 2004; Fuhler et al., 2005). Future experiments examining degranulation of eosinophils and neutrophils derived from TEL-Syk mice would provide insight into whether dysplastic myelopoiesis contributes to the inflammatory cytokine signature seen in MPN/MDS mouse models.

Induction of myeloproliferation with myelofibrosis has also been observed with other tyrosine kinases fused to TEL. In particular, the TEL-Lyn fusion, originally isolated from a patient with idiopathic myelofibrosis (Tanaka et al., 2010), retrovirally transduced into mouse fetal liver hematopoietic progenitors also leads to an aggressive MPN with excessive bone marrow fibrosis, culminating in lethality by 60 – 90 days following cell

transfer (Takeda et al., 2011). As we observed with TEL-Syk, the kinase inactive version of TEL-Lyn fails to induce hematopoietic progenitor proliferation, indicating the requirement for kinase activity in both models. Similarly, activation of STAT5 is observed in progenitors transduced with TEL-Lyn and development of myeloproliferative disease is prevented in Stat5-deficient mice. TEL fusion proteins with other tyrosine kinases, such as ABL1, ABL2, JAK2, NTRK3, FFGR3, and PDGFRB, have also been associated with various hematologic malignancies (Bohlander, 2005; Kuno et al., 2001), though direct comparisons between these fusion proteins in mouse models is not complete. Recent evidence demonstrated that BCR-ABL circumvents JAK2 and drives STAT5 signaling independently of cytokines in the context of CML (Hantschel et al., 2012). Hantschel et al. revealed that BCR-ABL induces CML in JAK2-deficient hematopoietic stem cells and causes STAT5 phosphorylation. Administration of various JAK2 inhibitors failed to block phosphorylation of STAT5 in Ba/F3 cells transduced with BCR-ABL. These results are consistent with our *in vitro* data demonstrating that TEL-Syk drives phosphorylation of STAT5 and colony formation in fetal liver cells even in the presence of JAK inhibitors. Mechanistically, it is evident that these fusions (BCR-ABL, TEL-Lyn, and TEL-Syk) uncouple the JAK2-STAT5 pathway for disease progression.

Overall, these results demonstrate that expression of the TEL-Syk fusion protein in fetal liver hematopoietic cells leads to rapid myeloproliferation and fatal myelofibrosis in a mouse model. The extent and the aggressive nature of this disease is unusual and will serve as a useful model for studying deregulated signaling in the context of myeloproliferative neoplasms with myelofibrosis. Future work with this model may

allow identification of the soluble factor(s) derived from the proliferating myeloid cells that contribute to the extensive stromal fibrosis. Though many investigators have implicated myeloid cell-derived factors in myelofibrosis, none have been defined.

CHAPTER FOUR

REGULATORY TYROSINES IN INTERDOMAIN B MEDIATE ADAPTOR FUNCTIONS IN SYK

4.1 INTRODUCTION

Tyrosine phosphorylation plays a pivotal role in kinase activation and adaptor function. Of the ~30 tyrosine residues that exist in Syk, 9 tyrosines (Fig 4.1 A) have been intensely characterized. Autophosphorylation of Y130, which resides between the two SH2 domains in Syk, reduces binding affinity of the two Syk SH2 domains for doubly phosphorylated ITAMs (Zhang et al., 2008). Phosphorylation of Y317 within the interdomain B, proximal to the C-terminal SH2 domain, of both ZAP-70 and Syk mediates ubiquintination by RING finger (RF) E3-ubiquitin ligase c-Cbl, which targets Syk and ZAP-70 for proteosomal degradation (Paolini et al., 2002). Deficiency and mutations in c-Cbl has been associated in a number of human myeloid malignancies, presumably due to sustained tyrosine kinase signaling and adaptor functions (Kales et al., 2010). Recent evidence has highlighted the importance of Y317 in osteoclast function, in which cytoskeletal rearrangement was altered in *syk*$^{-/-}$ osteoclast expressing Y317F (Zou et al., 2009). Kinase activity was unperturbed, while c-Cbl mediated ubiquination was reduced and enhanced cytoskeletal function. Furthermore, phosphorylation of Y317 enables P-I3K association, suggesting Y317 retains a scaffolding role in addition to facilitating protein turnover (Moon et al., 2005). Perturbation in phosphorylation of Y130 and Y317 leads to sustained Syk signaling, demonstrating the importance of the tyrosine residues in Syk regulation.

Interdomain B Y342, 346; activation loop Y519, 520; and C-terminal tyrosines Y623, 624, 625 mediate autoinhibition and facilitate association to downstream adaptor proteins. Based on ZAP-70 structural studies, in an inactive state hydrophobic residues in interdomain A of Syk make a pocket for insertion Y342, 346 that is further stabilized by residues in the kinase domain. Aromatic interactions between interdomain A, Y342, 346, and kinase domain is termed a "linker-kinase sandwich". Upon autophosphorylation of Y342, 346, this linker-kinase sandwich is disrupted allowing Syk to open up and active (Deindl et al., 2007). At 342 and 346, tyrosine-to-phenylalanine mutations impair calcium mobilization, degranulation, and phosphorylation of ERK1/2, Akt, and LAT in mast cells (Simon et al., 2005). In addition association and phosphorylation of Vav and PLC-γ are reduced, suggested that Y342 and Y346 are binding sites for Vav and PLC-γ. Indeed in studies examining Y342 and Y346 in B cells, tyrosine-to-phenylalanine mutations blunt calcium mobilization and binding of Vav SH2 domain (Chen et al., 2011; Kulathu et al., 2009).

Phosphorylation of Y519, 520 stabilizes the ATP and substrate-binding pockets that are necessary for high affinity FcεRI activation (Zhang et al., 2000). Upon cross-linking of FcεRI Y(519, 520)F Syk mutants expressed in *syk*$^{-/-}$ RBL-2H3 cells demonstrate normal phosphorylation as compared to wild-type controls, but have reduced degranulation as determined by histamine release (Zhang et al., 1998). Analogous mutations in ZAP-70 ablate kinase activity, demonstrating differences between the two kinases (de Castro, 2011).

Based on ZAP-70 structural studies, carboxyl-terminal tyrosines maintain a closed conformation in this family of tyrosine kinases by interacting with residues in the kinase

domain and interdomain B. Furthermore, phosphorylation of Y624, 625 facilitates SLP-76 and TULA-2 association (de Castro et al., 2012). SLP-76, in mast cells, and SLP-65, in B cells, are scaffolding proteins that enable recruitment and complex formation between Syk, Grb2, LAT, Nck, BTK and carboxyl terminal tyrosines in Syk (Kulathu et al., 2008). TULA-2 dephosphorylates SFKs and Syk and negatively regulates Syk function as seen in platelets downstream of GPVI signaling (Thomas et al., 2010). Disruption of tyrosines 342, 346, 519, 520, 624, 623 contributes to an open and active confirmation, and alters binding of downstream adaptors that are necessary for calcium mobilization and degranulation.

All of these mutations involve a tyrosine-to-phenylalanine substitution, suggesting that bulky residue substitutions facilitate conformational changes. Brdicka et al. demonstrated that a tyrosine-to-alanine mutation at Y315, 319 in ZAP-70 exaggerated TCR-induced NFAT activation as well enhanced phosphorylation. Analogous mutations in Syk, Y342, 346 led to enhanced phosphorylation of downstream adaptor NTAL (Brdicka et al., 2005). Previous studies demonstrated that alteration in these tyrosines did not affect phosphorylation by Syk; thus, we hypothesized that Y(342, 346)A would substitutions render Syk constitutively activate thus leading to deregulated downstream signaling.

4.2 RESULTS

4.2.1 Syk Y(342, 346)A leads to constitutive phosporylation of NTAL and other cellular targets

Syk and ZAP-70 demonstrate homology at a number of key regulatory residues, specifically within the YESPY amino acid sequence (Figure 4.1 B). Using site-directed

mutagenesis, a Syk Y(342, 346)A mutant was generated and assessed for constitutive activation as performed by Brdicka et al. HEK293 cells were transiently co-transfected with NTAL, a downstream target, and vector alone, Syk, TEL-Syk, and Syk Y(342, 346)A, and then examined for total tyrosine phosphorylation and NTAL phosphorylation. In the absence of upstream SFK activation only TEL-Syk and Syk Y(342, 346)A lead to both global tyrosine phosphorylation and phosphorylation of NTAL (Fig 4.1 C), while Syk did not demonstrate a robust phosphorylation of NTAL. Based on evidence provided in Chapter 3 that TEL-Syk is constitutively active, global tyrosine and NTAL phosphorylation suggests that Syk Y(342, 346)A is also constitutively active.

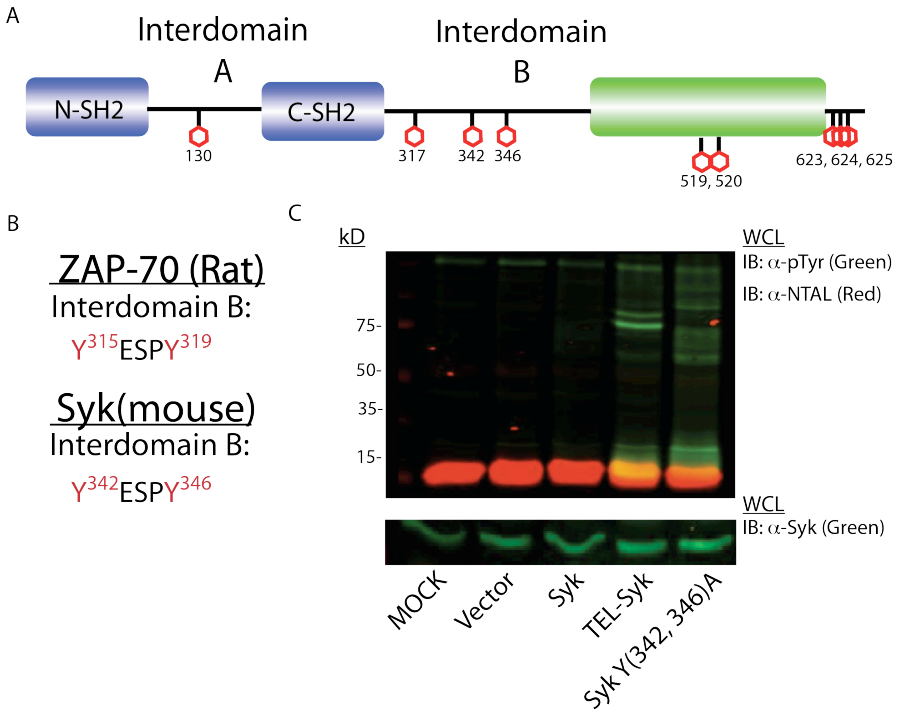

Figure 4. 1 Tyrosine to alanine subsitution at tyrosines Y342 and Y346 lead to constitutive NTAL phosphorylation, (A) A schematic of Syk protein (B) Interdomain B tyrosines and homology between mSyk and rZAP-70 (C) NTAL phosphorylation in HEK293 cells transiently co-transfected with vector, Syk, TEL-Syk, and Syk Y(342, 346)A and NTAL

4.2.2 Syk Y(342, 346)A does not lead to enhanced autophosphorylation

We next hypothesized that constitutive phosphorylation is due to enhanced autophosphorylation. To answer this question, we conducted an *in vitro* kinase assay. HEK293 cells were transiently transfected with vector, Syk, TEL-Syk and Syk Y(342, 346)A, immunoprecipitated and assessed for P^{32} incorporation as a read-out for autophosphorylation. In Figure 4.2 A, Syk Y(342, 346)A did not demonstrate an increase in autophosphorylation as compared to Syk and TEL-Syk, and instead revealed similar autophosphorylation levels as vector alone. However, examination of the immunoprecipitates (Fig. 4.2 A lower panel) revealed that Syk Y(342, 346)A species were phosphorylated as determined by 4G10 immunoblotting for pTyr. In Figure 4.2 B quantitation of P^{32} incorporation demonstrated that Syk Y(342, 346)A had ~20% decrease in autophosphorylation compared to Syk. The data indicates that Syk Y(342, 346)A phosphorylates NTAL and other cellular targets, but does not incorporate radiolabeled ATP.

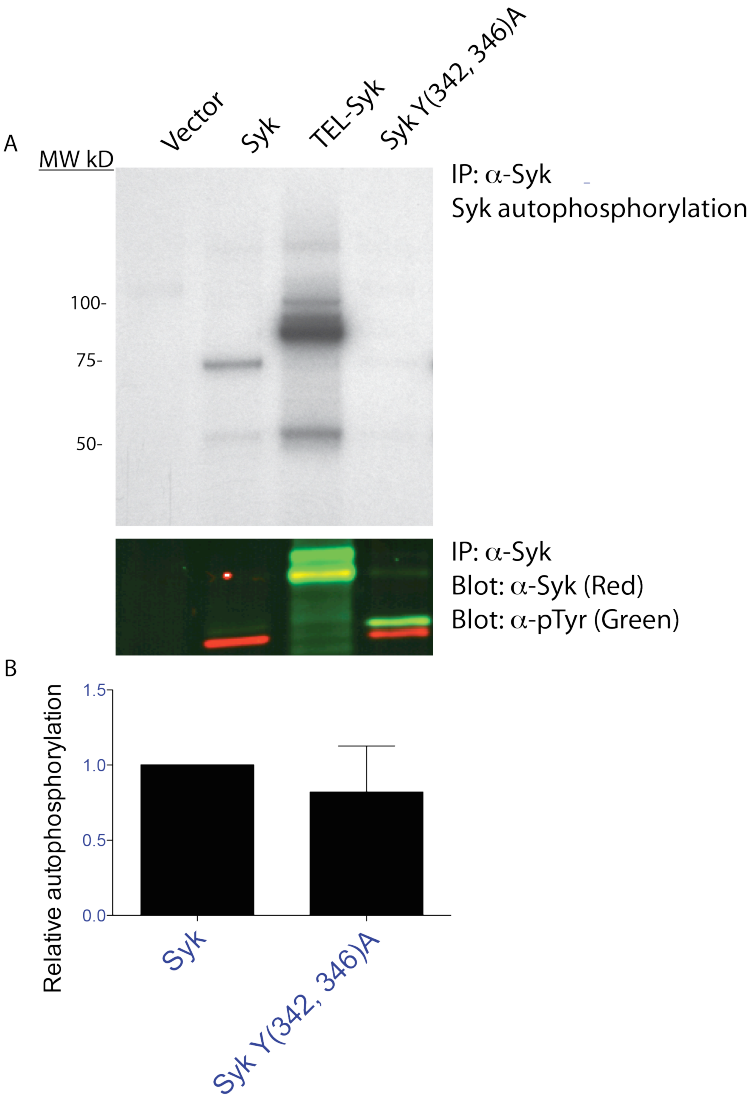

Figure 4. 2 Syk Y(342, 346)A fails to autophosphorylate. (A) Autophosphorylation of Syk Y(342, 346). HEK293T cells were transiently transfected with empty vector, Syk, TEL-Syk, and Syk Y(342, 346) A. For the *in vitro* kinase assay, cell lysates were immunoprecipitated with anti-Syk then incubated with P^{32} labeled ATP. Immunoblots showing levels of, Syk in red and pTyr in green are shown below autoradiogram. (B) Quantitation of autophosphorylation by Syk and Syk Y(342, 346)A. Values were a ratio of normalized intergrate density value to normalized intensity fluorescent values.

4.2.3 Syk Y(342, 346)A lead to normal phagocytosis, but blunts calcium mobilization and transformation

We assessed whether global tyrosine phosphorylation of cellular targets in the presence of Syk Y(342, 346)A led to dysfunctional cellular responses. In order to test this hypothesis, we examined Syk Y(342, 346)A effect on Fc receptor-mediated

phagocytosis, BCR-mediated calcium flux, and transformation of Ba/F3 cells. Fc receptors bind to IgG molecules that coat target particles such as microbes, tumors, and non-self tissue. The uptake of these IgG-opsonized particles is dependent on Syk. Taking advantage of Syk-dependent Fc-mediated phagocytosis, we retrovirally transduced BMDMs with Syk and Syk Y(342, 346)A as assessed for internalization of IgG-opsonized SRBCs. As previously described, *syk*$^{-/-}$ BMDMs fail to phagocytose IgG-opsonized SRBCs, while both controls, Syk reconstituted *syk*$^{-/-}$ BMDMs and WT BMDM, similarly phagocytose IgG-opsonized SRBCs (Fig 4.3 A). Syk Y(342, 346)A internalized IgG-opsonized SRBCs similarly to controls, suggesting that neither constitutive phosphorylation and Y(342, 346)A substitution alters phagocytosis.

Syk transmits signals downstream of the BCR upon ligation that leads to phosphorylation of PLC-γ and $InsP_3$ generation. $InsP_3$ then activates calcium channels on the endoplasmic reticulum that allow the flow of calcium from intracellular stores in the cytoplasm for further cellular activation. To determine if Syk Y(342, 346)A affects the calcium mobilization, we retrovirally transduced vector, Syk, and Syk Y(342, 346)A into *syk-/-* DT-40 cells, chicken B cell line, then followed calcium release into the cytoplasm after BCR cross-linking using the calcium indicator dye Indo-1. As compared to WT and Syk DT-40 cells, Syk Y(342, 346)A failed to induce calcium mobilization upon BCR cross-linking (Fig 4.3 B) and resembled the non-existent calcium response of vector, suggesting that Y(342, 346)A substitution alters Syk mediated calcium mobilization.

In chapter 3, we demonstrated that constitutively active TEL-Syk leads to enhanced NTAL phosphorylation as well as deregulated signaling. Previous data also revealed that TEL-Syk led to growth of Ba/F3 cells in the absence of the growth factor

IL-3. Syk Y(342, 346)A mutant was retrovirally transduced into Ba/F3 cells and assessed transformation or growth in the absence of IL-3. In Figure 4.3 C, Syk Y(342, 346)A did not transform Ba/F3 cells as compared to TEL-Syk, and demonstrated a similar growth pattern as IL-3 treated Ba/F3 cells and vector and Syk expressing Ba/F3 cells. In data not shown, we also assessed whether Syk Y(342, 346)A led to hypersensitivity to low cytokine stimulation and discovered that Syk Y(342, 346)A does not similarly enhance colony-formation as compared to TEL-Syk (Fig 3.1 C) in the presence of low cytokine levels.

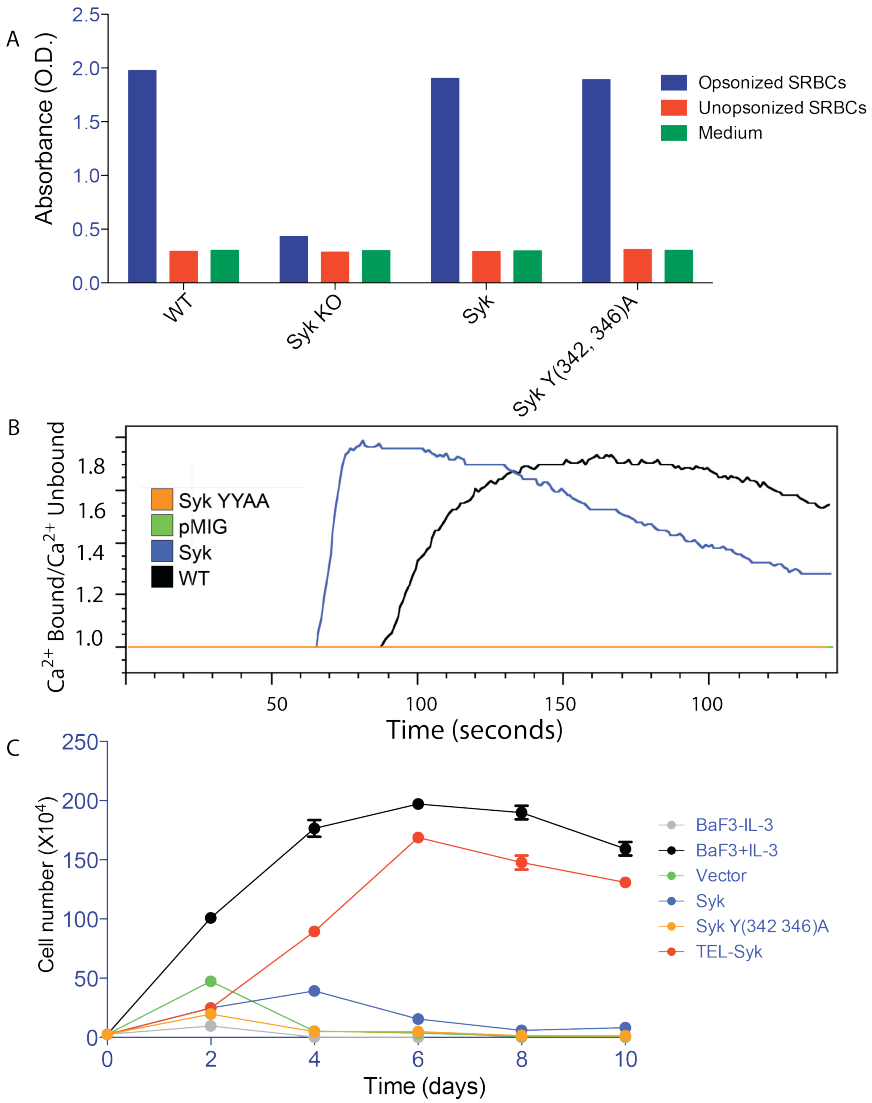

Figure 4. 3 Syk Y(342, 346)A phagocytoses opsonized sheep red blood cells, but fails to mobilize calcium and transform Ba/F3 cells. (A) Phagocytosis of opsonized sheep red blood cells in *syk*$^{-/-}$ bone-marrow derived macrophages. Bone marrow from syk-/- chimeras were retrovirally transduced with Syk and Syk Y(342, 346)A, sorted for GFP, and culture in media containing GM-CSF. Cells were incubated with IgG opsonized sheep red blood cells for 1hr. (B) Calcium mobilization after BCR cross-linking. DT-40 B-cells were retrovirally transduced with vector, Syk, and Syk Y(346,342)A, sorted for GFP, and then stimulated with chicken α-IgM. Calcium mobilization was measure on a LSRII using a UV laser. (C) IL-3 independent growth in Ba/F3 cells. Ba/F3 murine hematopoietic cells were retrovirally transduced with vector, Syk, TEL-Syk, and Syk Y(342, 346)A, sorted for GFP, and culture in media without IL-3, unless indicated. Cell numbers were enumerated on days 2, 4, 6, 8, and 10.

4.3 Discussion

In this study, our aim was to determine whether Syk Y(342, 346)A would lead to constitutive activation and deregulated function. We demonstrated that Syk Y(342, 346)A robustly phosphorylates NTAL, but fails to induce calcium mobilization, growth factor independence, and autophosphorylation. Enhanced tyrosine phosphorylation and reduced incorporation of radiolabeled ATP by the *in vitro* autophosphorylation assay in Syk Y(342, 346)A suggests that Y342, 346 residues play a major role in Syk function and are main sites for autophosphorylation. We can speculate that during Syk activation that Y342, 346 are autophosphorylated and phosphorylation of other tyrosine residue may depend more on extrinsic *cis*- or *trans*-phosphorylation, i.e. activation of Syk leads to phosphorylation of tyrosines on neighboring Syk species.

Tyrosine residues 342 and 346 are not only involved in autoregulation of kinase activity, but also binding to downstream mediators Vav, PLC-γ2, Grb2, and others. PLC-γ2 mediates downstream calcium mobilization by generating $InsP_3$ that binds to ion channels in the endoplasmic reticulum, releases calcium into the cytoplasm and subsequently activates STIM1. STIM1 then homo-dimerizes and activates CRAC channel proteins, located on the plasma membrane, that mediate extracellular influx of calcium (Soboloff et al., 2012). Ablated binding of PLC-γ2 to mutated Y342/346 reduces activation PLC-γ2 and calcium mobilization. In fact, PLC-γ2-deficient mast cells demonstrate normal MAPK activation and cytokine production, but reduced calcium influx and $InsP_3$ production downstream of FcγR and FcεR (Wen et al., 2002). Moreover, PLC-γ2-deficient B-cells demonstrated reduced calcium mobilization and T cell-

independent antibody production (Wang et al., 2000). It is likely that BCR cross-linked Syk Y(342, 346)A DT-40 cells fail to associate with PLC-γ2 and promote calcium mobilization.

As for the failure to transform to Ba/F3 cells, Syk Y(342, 346)A does not have the same catalytic strength as TEL-Syk as seen in Figures 4.1C and 4.2A. Furthermore, since Syk Y(342, 346)A contains two SH-2 domains, while TEL-Syk does not, Syk Y(342, 346)A may be sequestered to other areas of the cell that are not proximal to growth/survival pathways as TEL-Syk. Indeed, Kanie et al. (Kanie et al., 2004) demonstrated that TEL-Syk is almost entirely cytoplasmic.

CHAPTER FIVE

MUTATIONS IN REGULATORY MOTIFS LEADS TO CONSTITUTIVE ACTIVATION OF SYK

5.1 INTRODUCTION

Syk plays an essential role in modulating survival, proliferation, differentiation and effector signals downstream of immune receptors. Deregulation of the signaling pathways governed by Syk leads to not only hematopoietic malignancies, but also autoimmunity in humans and mice. Lyn, a Src-family kinase, works upstream of Syk in immune receptor signaling, and in a gain-of-function mutant model ($Lyn^{up/up}$), mice develop elevated levels of IgM and IgG, glomerulonephritis and malformed spleens and lymph nodes (Hibbs et al., 2002). Biochemical analysis of Syk and other signaling mediators reveals that Syk is constitutively phosphorylated independent of immune receptor ligation; an indication that constitutive activation of Syk correlates with autoimmunity. Second, the motheaten viable (me^{v}) mouse model, a missense mutation in the *shp-1* gene that results in a subsequent deletion of the phosphatase catalytic domain, is characterized by myeloproliferation, extensive dermatitis, peritonitis and pneumonitis (Green and Shultz, 1975). A catalytically inactive form of SHP-1 leads to constitutive phosphorylation of Syk, a hallmark of activation (Dustin et al., 1999). Based on these findings, constitutive phosphorylation and activation of Syk may cause autoimmunity and inflammation, but this hypothesis has not been formally tested.

ZAP-70, a non-receptor protein tyrosine kinase that modulates TCR signaling, is regulated by auto-inhibitory motifs, and disruption of this regulatory mechanism leads to constitutive activation. Interdomain A, a short amino acid sequence between the two N-

terminus SH2 domains, and Interdomain B, a linker region between the C-terminus SH2 domain and the kinase domain, are chiefly thought to mediate ZAP-70 and Syk intramolecular auto-inhibition (Figure 5.1 A and B). Structural analysis of ZAP-70 Y315/319F mutant reveals that interdomain A interacts with residues in interdomain B as well as residues in the kinase domain (Deindl et al., 2007). From this study the authors postulate that a series of paired interactions -- L133 and W131 with Y315; Y319 with P396; Q145 and P147 with Y597 and Y598 -- stabilize ZAP-70 in an inactive conformation. Following receptor ligation and SFK phosphorylation of ITAM-associated adaptors, ZAP-70 binds to doubly phosphorylated ITAMs via the N-terminus SH2 domains and leads to Y315, 319 phosphorylation. Y315, 319 phosphorylation energetically disrupts the paired interactions between these tyrosines, a hydrophobic pocket generated by interdomain A, and the kinase domain; this ultimately relieves auto-inhibition. Since ZAP-70 and Syk are highly homologous especially at these regulatory regions, it is reasonable to assume that similar regulatory mechanisms govern Syk activation, such that mutations in interdomains A and B and the kinase domain will lead to Syk constitutive activation, deregulated signaling and altered downstream immune functions.

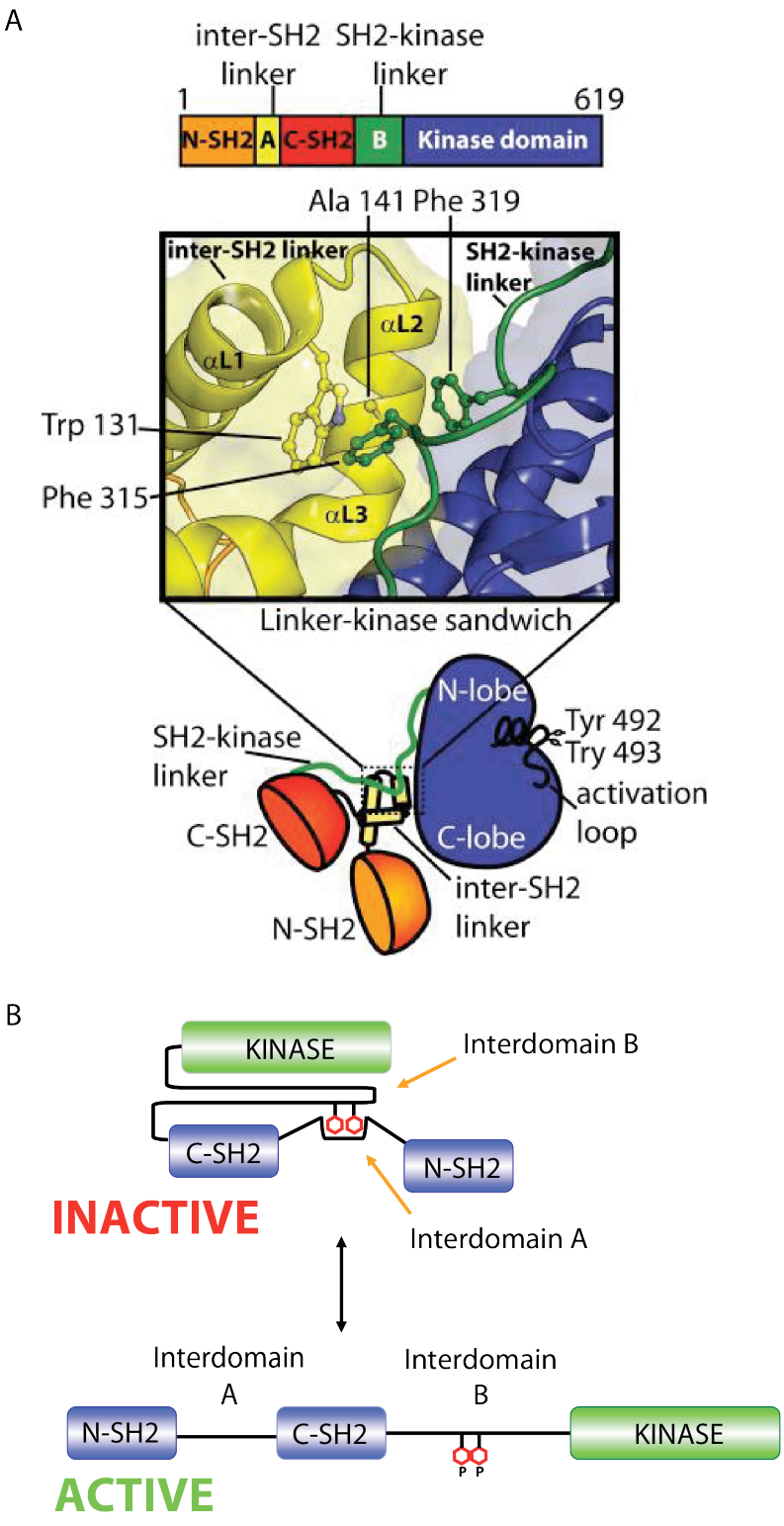

Figure 5. 1 Non-receptor tyrosine kinase autoinhibition and activation (A) Schematic of ZAP-70 autoinhibition (Deindl et al., 2009) (B) schematic of Syk activation

5.2 RESULTS

5.2.1 Generation of Allelic Series in Syk

Remarkably, key regulatory residues are conserved between rat ZAP-70 and mouse Syk and suggest an evolutionary pressure to retain these residues in Syk and ZAP-70 in order to regulate immunoreceptor signal transduction. Based on ZAP-70 crystal structure and mutagenesis studies, we predict that residues W135, L137, A145, S148, Q149 and P151 in interdomain A and Y623 in the C-terminus of the kinase domain are critical in maintaining Syk autoinhibition in the absence of upstream signaling. To address the question of whether disrupting residues in the key regulatory motifs in Syk leads to deregulating signaling, we generated an allelic series, by site-directed mutagenesis, in which indicated (Fig. 5.2 A and B) residues were mutated to either alanine or glutamic acid.

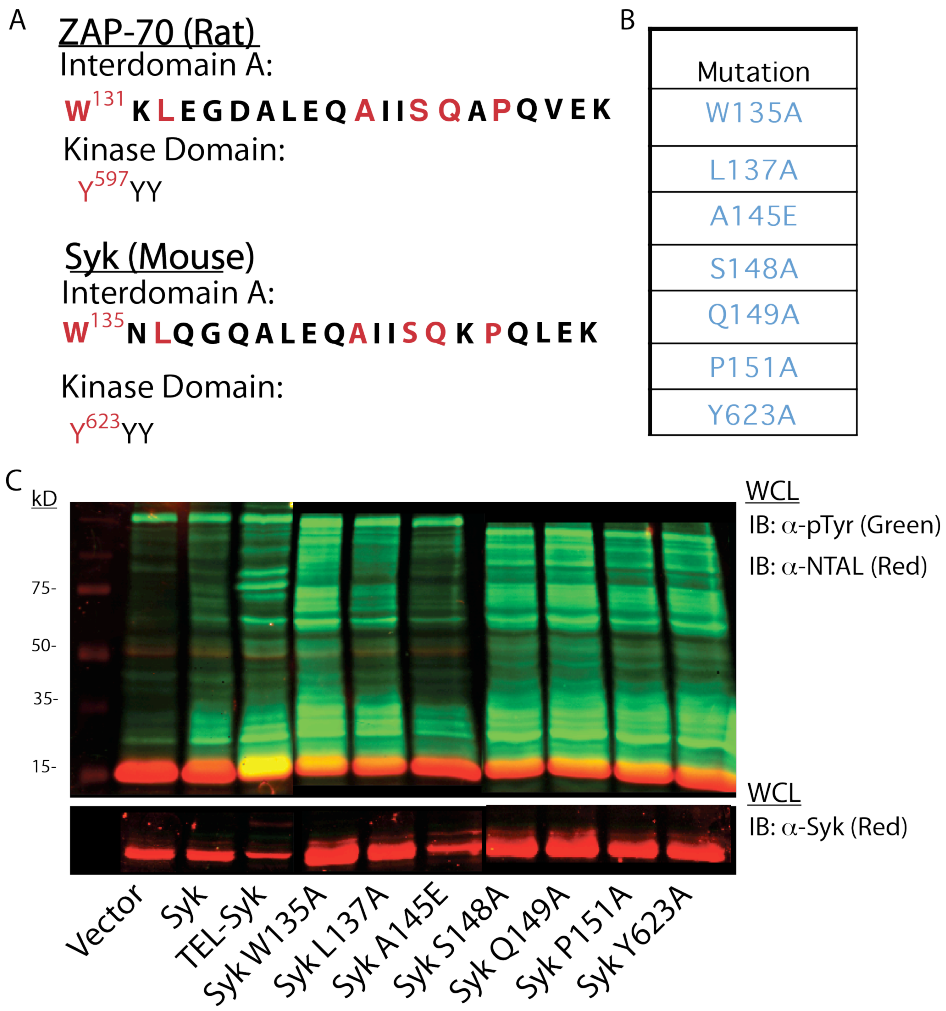

Figure 5. 2 Mutagenesis of residues in regulatory motifs leads to constitutive activation (A) Amino acid sequence of rZAP-70 and mSyk in interdomain A and C-terminal tail. (B) Amino acid subsitutions made in mSyk by site-directed mutagenesis and cloned into the pMIG expression vector. (C) NTAL phosphorylation in HEK293 cells. HEK293 cells were transiently co-transfected with NTAL and Syk mutants. Immunoblot analysis for NTAL (red) and pTyr (Green and Shultz). Expression level of Syk mutants in lower panel (red) by immunoblot analysis.

In order to determine constitutive activation, we co-transfected NTAL, a LAT homolog, and Syk mutants into HEK293 cells and examined by immunoblot analysis for total tyrosine and NTAL phosphorylation. In the absence of SFK signaling, which is needed to promote wild-type Syk activation, TEL-Syk, the positive control, phosphorylated NTAL, while NTAL phosphorylation was absent in Syk in transduced cells (Fig. 5.2 C). W135A, L137A, and P151A demonstrated NTAL phosphorylation as well as increased

tyrosine phosphorylation compared to Syk alone. To determine if increased phosphorylation was due to expression level of the mutant Syk protein, we assessed the expression of Syk by immunoblot analysis and found all Syk variants were expressed at similar levels, arguing that expression did not affect phosphorylation.

5.2.2 Increased autophosphorylation occurs in W135A and Q149A mSyk mutant, but is reduced in S148A

We next assessed autophosphorylation in Syk mutants using an *in vitro* autophosphorylation assay to investigate whether constitutive activity leads to autophosphorylation. Incorporation of radiolabeled P^{32} was robustly observed in control kinase TEL-Syk and weakly found in Syk transfected HEK293 cells in the absence of upstream SFK activation (Fig. 5.3 A). W135A and Q149A Syk mutants showed greater autophosphorylation than Syk alone (Fig 5.3 A and B). S148A demonstrated a 20-30% decrease, respectively, in autophosphorylation compared to Syk, while W135A and Q149A revealed a 40-80% increase, respectively, compared to Syk. Syk A145E and L137A were either undetectable or demonstrated low expression multiple times, thus it was difficult to determine autophosphorylation.

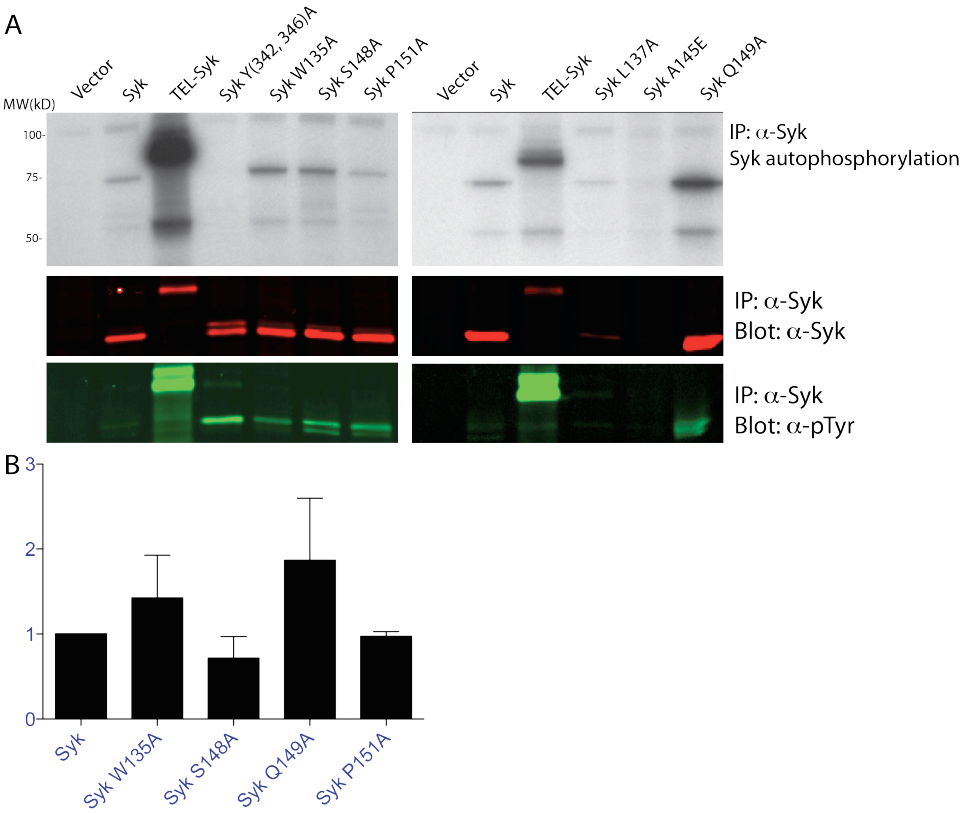

Figure 5. 3 Autophosphorylation of Syk mutants (A)utophosphorylation of Syk mutants. HEK293T cells were transiently transfected with empty vector, Syk, TEL-Syk, and Syk mutants. For the *in vitro* kinase assay, cell lysates were immunoprecipitated with anti-Syk then incubated with P^{32} labeled ATP. Immunoblots showing levels of, Syk in red and pTyr in green are shown below autoradiogram. (B) Quantitation of autophosphorylation by Syk mutants. Values were a ratio of normalized intergrate density value to normalized intensity fluorescent values.

5.2.3 Syk mutants did not lead to enhanced calcium mobilization or growth factor-independent growth

Calcium mobilization from the endoplasmic reticulum is mediated by a Syk-PLC-γ2-IP_3 axis that activates store operated calcium channel protein STIM1 in B-cells after BCR engagement by cognate antigen; thus, calcium mobilization is a read-out for B-cell activation and subsequent Syk activation. To assess for exaggerated Syk function, we retrovirally introduced Syk mutants into Syk-deficient DT-40 cells (a chicken B-cell line) then and sorted for GFP^+ DT-40 cells. Previously studies examining Lyn-deficient B-cells, which have increased Syk phosphorylation, revealed that low dose administration of α–IgM robustly increased calcium mobilization compared to wild-type control

suggesting that constitutively active Syk mutants would lead to an exaggerated calcium mobilization in stimulated chicken B-cells. Syk mutant DT-40 cells were treated with a low dose of chicken α-IgM, 500ng/mL, then and assessed for calcium binding to Indo-1, a calcium indicator. In panel A of Figure 5.4, wild-type control DT-40 cells had a steady increase and then gradual decrease in calcium mobilization over time, while Syk reconstituted DT-40 showed an initial sharp peak and then a gradual reduction in calcium signal. In comparison, P151A closely mimicked Syk calcium mobilization after α-IgM stimulation. The remaining Syk mutants demonstrated a muted and intermediate calcium signal compared to Syk and wild-type controls.

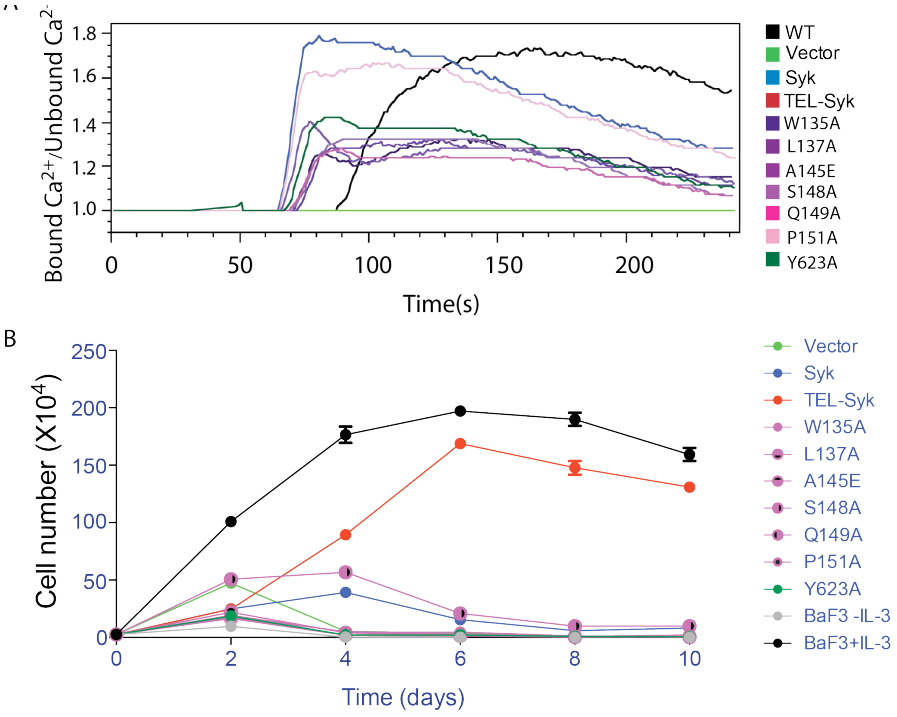

Figure 5. 4 Reduced calcium and growth responses of Syk mutants. .(A) Calcium mobilization after BCR cross-linking. DT-40 B-cells were retrovirally transduced with vector, Syk, and Syk mutants, sorted for GFP, and then stimulated with chicken α-IgM. Calcium mobilization was measure on a LSRII using a UV laser. (B) IL-3 independent growth in Ba/F3 cells. Ba/F3 murine hematopoietic cells were retrovirally transduced with vector, Syk, TEL-Syk, and Syk mutants, sorted for GFP, and culture in media without IL-3, unless indicated. Cell numbers were enumerated on days 2, 4, 6, 8, and 10

To further assess for Syk-mediated alternations is cellular activation and function, we examined the growth potential of Syk mutants in a mouse hematopoietic cell line, Ba/F3, in the presence or absence of growth factor stimulation, IL-3. Ba/F3 cells have been used to discriminate the oncogenic potential of numerous hematopoietic-derived fusion proteins, among them TEL-Syk. Ba/F3 cells were retrovirally transduced with TEL-Syk, Syk and Syk allelic mutants and sorted for GFP^+ expression. As expected, TEL-Syk induced growth in absence of IL-3, and reproduced the previously published result (Fig. 5.4 B). Syk as well as Syk mutants did not lead to growth factor independent growth as seen in both Ba/F3 cells treated with IL-3 and the TEL-Syk control. Given that transformation of Ba/F3 may need a strong oncogenic stimulus, we further examine the hypersensitivity of these Syk mutants to varying levels of GM-CSF in a colony-forming assay. Unfortunately, none of the Syk mutants demonstrated hypersensitivity to low GM-CSF (data not shown) as demonstrated in TEL-Syk colony-forming assays (Fig. 3.1 C).

5.3 Discussion

In this study, our aim was to determine whether mutations in regulatory motifs of Syk would lead to constitutive activation and deregulated function. Variable calcium mobilization and autophosphorylation in Syk mutants --W135A and Q149A have increased autophosphorylation and most Syk mutants are hypomorphic for calcium mobilization after BCR cross-linking -- suggests that although several mutants are constitutively active, compensatory mechanism are preventing deregulated signaling. NTAL phosphorylation and Syk autophosphorylation were performed in HEK293 cells and the epithelial cytoplasmic environment is vastly different from an immune cell cytoplasm. Association of c-Cbl at phosphorylated Y317 in interdomain B may

compensate for deregulated Syk activity by targeting the constitutively active mutants to the proteosome for degradation. The importance of Y317 is highlighted in studies investigating Syk function in osteoclasts, DT-40s and the mast cell line RBL-2H3. Furthermore, the TEL-Syk fusion does not retain a c-Cbl binding site and thus is refractory to ubiquitin-mediated degradation. It would be interesting to assess the relative ubiquitination in Syk mutants in both DT-40 and Ba/F3 cells and subsequent degradation. Such experiments would provide insight into how constitutive activation upregulates compensatory mechanisms, like c-Cbl-mediated protein degradation, and prevents deregulated downstream activation and function.

SHP-1 is another attractive regulator that may attenuate deregulated signaling by Syk mutants. SHP-1 is a phosphatase that binds to ITIMs, or immunoreceptor tyrosine-based inhibitory motifs, on regulatory receptors and dephosphorylates signaling molecules such as Syk. SHP-1 associates with Syk in splenic B cells (Dustin et al., 1999). SHP-1 C453S, a dominant negative variant with ablated phosphatase activity, was then introduced into a B-cell lymphoma line and assessed for Syk phosphorylation and calcium mobilization after BCR cross-linking. SHP-1 C453S increases Syk phosphorylation and exaggerates calcium mobilization, revealing that SHP-1 modulates Syk activity downstream of BCR signaling. Furthermore, overexpression of SHP-1 in a macrophage cells line J774A.1 abrogates Fc receptor-mediated phagocytosis, but the authors failed to assess Syk dephosphorylation (Kant et al., 2002). Evidence for SHP-1 regulation of phagocytosis in macrophages has been further parsed by investigation of the CD47-SHPS-1/SIRPα pathway (Okazawa et al., 2005). SIRPα mutant peritoneal elicited macrophages and siRNA knockdown of SIRPα in macrophages enhance Fc receptor-

mediated phagocytosis. Inhibitors against Syk and PI3K ablated enhancement of phagocytosis in SIRPα deficient macrophages, although phosphorylation of Syk and P13K were normal in SIRPα deficient macrophages after FcγR stimulation. A potential future experiment would be to assess for the association of SHP-1 as well as other phosphatase with Syk mutants and whether sodium stibogluconate, an SHP-1 inhibitor, treatment enhances calcium mobilization. These experiments would provide some evidence that SHP-1 and other phosphatases tightly modulate Syk activity and prevent deregulated signaling.

Lastly, overexpression of Syk mutants in either DT-40 or Ba/F3 cells may be toxic. It would be interesting to analyze phosphorylation states of various downstream signaling molecules such as PLC-γ, Vav, Akt, SLP-76/SLP-65, Erk1 and Erk2, etc. This would provide insight into whether mutations in residues that mediate Syk inhibition do indeed lead to deregulated signaling. Furthermore, analysis of apoptotic pathways might also provide a rationale for why Syk gain-of-function mutations lead to hypomorphic responses regardless of constitutive activation.

CHAPTER SIX

CONCLUSION

Syk mediates signaling downstream of multiple immunoreceptors and facilitates activation, survival, growth, and effector immune functions. As a critical mediator of receptor signaling, Syk overexpression and disruption of regulator mechanism often lead to myeloid malignancies and autoimmunity. Intrinsic and extrinsic regulation is vital in preventing disease development and progression.

TEL-Syk, a fusion protein that contains the protein oligomerzation domains of TEL and a short stretch of interdomain B and the kinase domain of Syk, leads to constitutive activation and hypersensitivity to low cytokine level. Introduction of the TEL-Syk into fetal liver hematopoietic cells reduced survival of chimeric mice and expanded cells from the myeloid lineage, specifically neutrophils, monocytes, and eosinophils. Dysmyelopoiesis, dyserythropoiesis and fibrosis of the spleen and bone marrow revealed that TEL-Syk leads to a myeloproliferative neoplasm with myelodysplastic features. We further demonstrated that, similar to human MPNs and MDS, TEL-Syk chimeras elevate circulating proinflammatory cytokines. We also discovered that STAT5 plays a role in TEL-Syk deregulated signaling and hypersensitivity to low cytokines. MPN development was blocked in TEL-Lyn on a STAT5 deficient background (Takeda et al., 2011). A proof-of-principle experiment would be to retrovirally transduce STAT5 deficient fetal liver hematopoietic cells with TEL-Syk and assess for MPN development. Deficiency in STAT5 should block MPN development. Other remaining questions are whether dysplasic myeloid cells are

reservoirs for proinflammatory cytokines and whether premature release is due to deregulated degranulation. Furthermore, what is the reaction of the stromal microenvironment to TEL-Syk deregulated signaling in fetal liver hematopoietic cells? What are the players or mechanisms that lead to bone marrow fibrosis during TEL-Syk deregulating signaling? Are TEL-Syk HSCs in a non-quiescent cycling state with an expansion in CMP and GMP populations?

Disruption of autoregulatory regions either through Syk Y(342, 346)A substitution or mutagenesis of residues necessary for autoinhibition of Syk lead to enhanced NTAL phosphorylation and tyrosine phosphorylation. We did not see any functional change in DT-40 cells or mouse Ba/F3 expressing Syk Y(342, 346)A mutants. Although it is apparent that Syk autophosphorylated Y342 and 346, phosphorylation of other tyrosine residues without upstream activation suggests that Syk could phosphorylate other proteins beside PLC-γ2. A straight-forward experiment would be to assess phosphorylation of STAT5, the MAPK pathway, and c-Cbl in Ba/F3 cells in the absence of IL-3 stimulation. This would reveal that although Syk does not transform Ba/F3 cells, deregulated signaling may still be occurring. Second, we could also assess the relative contribution of compensatory mechanisms that neutralize Syk mutant constitutive activation. It is also important to assess whether Syk still associates with PLC-γ2 and thereby verifying that Y342, 346 is indeed necessary for PLC-γ2 association and initiation of calcium flux after BCR engagement.

Overall, this body of work provides further insight into deregulated Syk signaling and that TEL-Syk leads to a myeloid proliferative neoplasm with fibrosis rather than a lymphoid leukemia as previously published. TEL-Syk is yet another example of how

fusion proteins, like BCR-ABL and TEL-Lyn, circumvent JAK2 signaling and induce STAT5 activation; thus, mimicking *JAKV617F* deregulated signaling. The emerging paradigm that tyrosine kinase-containing fusion proteins directly phosphorylated STAT5 independent of JAK2 activation demonstrates that treatment of MPNs with JAK inhibitors will be inefficacious in *JAK2 V617F*$^-$ cases. Treatment with pan-kinase inhibitors, such as Gleevec that indirectly inhibits Syk, for *JAK2 V617F*$^-$ MPNs with elevated tyrosine kinase activation might be an attractive strategy for diagnosis and therapy.

CHAPTER SEVEN

REFERENCES

Adams, G.B., and Scadden, D.T. (2006). The hematopoietic stem cell in its place. Nat Immunol *7*, 333-337.

Andreotti, A.H., Schwartzberg, P.L., Joseph, R.E., and Berg, L.J. (2010). T-cell signaling regulated by the Tec family kinase, Itk. Cold Spring Harbor Perspectives in biology *2*, a002287.

Bailet, O., Fenouille, N., Abbe, P., Robert, G., Rocchi, S., Gonthier, N., Denoyelle, C., Ticchioni, M., Ortonne, J.P., Ballotti, R.*, et al.* (2009). Spleen tyrosine kinase functions as a tumor suppressor in melanoma cells by inducing senescence-like growth arrest. Cancer Res *69*, 2748-2756.

Bohlander, S.K. (2005). ETV6: A versatile player in leukemogenesis. Sem Cancer Biol 167-174.

Boisset, J.C., and Robin, C. (2012). On the origin of hematopoietic stem cells: progress and controversy. Stem Cell Res *8*, 1-13.

Brdicka, T., Kadlecek, T.A., Roose, J.P., Pastuszak, A.W., and Weiss, A. (2005). Intramolecular regulatory switch in ZAP-70: analogy with receptor tyrosine kinases. Mol Cell Biol *25*, 4924-4933.

Buchner, M., Fuchs, S., Prinz, G., Pfeifer, D., Bartholome, K., Burger, M., Chevalier, N., Vallat, L., Timmer, J., Gribben, J.G.*, et al.* (2009). Spleen tyrosine kinase is overexpressed and represents a potential therapeutic target in chronic lymphocytic leukemia. Cancer Res *69*, 5424-5432.

Cain, J.A., Xiang, Z., O'Neal, J., Kreisel, F., Colson, A., Luo, H., Hennighausen, L., and Tomasson, M.H. (2007). Myeloproliferative disease induced by TEL-PDGFRB displays dynamic range sensitivity to Stat5 gene dosage. Blood *109*, 3906-3914.

Catlin, S.N., Busque, L., Gale, R.E., Guttorp, P., and Abkowitz, J.L. (2011). The replication rate of human hematopoietic stem cells in vivo. Blood *117*, 4460-4466.

Chen, C.H., Martin, V.A., Gorenstein, N.M., Geahlen, R.L., and Post, C.B. (2011). Two closely spaced tyrosines regulate NFAT signaling in B cells via Syk association with Vav. Mol Cell Biol *31*, 2984-2996.

Chen, L., Monti, S., Juszczynski, P., Daley, J., Chen, W., Witzig, T.E., Habermann, T.M., Kutok, J.L., and Shipp, M.A. (2008). SYK-dependent tonic B-cell receptor signaling is a rational treatment target in diffuse large B-cell lymphoma. Blood *111*, 2230-2237.

Coopman, P., Do, M., Barth, M., Bowden, E., Hayes, A., Basyuk, E., Blancato, J., Vezza, P., McLeskey, S., Mangeat, P.*, et al.* (2000). The Syk tyrosine kinase suppresses malignant growth of human breast cancer cells. Nature *406*, 742-747.

Costa, G., Kouskoff, V., and Lacaud, G. (2012). Origin of blood cells and HSC production in the embryo. Trends Immunol *33*, 215-223.

de Castro, R.O. (2011). Regulation and function of syk tyrosine kinase in mast cell signaling and beyond. J Signal Transduct *2011*, 507291.

de Castro, R.O., Zhang, J., Groves, J.R., Barbu, E.A., and Siraganian, R.P. (2012). Once phosphorylated, tyrosines in carboxyl terminus of protein-tyrosine kinase Syk interact with signaling proteins, including TULA-2, a negative regulator of mast cell degranulation. J Biol Chem *287*, 8194-8204.
Deindl, S., Kadlecek, T., Brdicka, T., Cao, X., Weiss, A., and Kuriyan, J. (2007). Structural basis for the inhibition of tyrosine kinase activity of ZAP-70. Cell *129*, 735-746.
Deindl, S., Kadlecek, T.A., Cao, X., Kuriyan, J., and Weiss, A. (2009). Stability of an autoinhibitory interface in the structure of the tyrosine kinase ZAP-70 impacts T cell receptor response. Proc Natl Acad Sci U S A *106*, 20699-20704.
Dierks, C., Adrian, F., Fisch, P., Ma, H., Maurer, H., Herchenbach, D., Forster, C.U., Sprissler, C., Liu, G., Rottmann, S.*, et al.* (2010). The ITK-SYK fusion oncogene induces a T-cell lymphoproliferative disease in mice mimicking human disease. Cancer Res *70*, 6193-6204.
Dong, S.W., Ma, L., Xu, N., Yan, H.Q., Liu, H.Y., Li, Y.W., and Zhang, P. (2011). Research on the reactivation of Syk expression caused by the inhibition of DNA promoter methylation in the lung cancer. Neoplasma *58*, 89-95.
Dustin, L.B., Plas, D.R., Wong, J., Hu, Y.T., Soto, C., Chan, A., and Thomas, M.L. (1999). Expression of dominant-negative Src-homology domain 2-containing protein tyrosine phosphatase-1 results in increased Syk tyrosine kinase activity and B cell activation. J Immunol *162*, 2717-2724.
Feldman, A., Sun, D., Law, M., Novak, A., Attygalle, A., Thorland, E., Rink, S., Vrana, J., Caron, B., Morice, W.*, et al.* (2008). Overexpression of Syk tyrosine kinase in peripheral T-cell lymphomas. Leukemia *22*, 1139-1143.
Fuhler, G.M., Cadwallader, K.A., Knol, G.J., Chilvers, E.R., Drayer, A.L., and Vellenga, E. (2004). Disturbed granulocyte macrophage-colony stimulating factor priming of phosphatidylinositol 3,4,5-trisphosphate accumulation and Rac activation in fMLP-stimulated neutrophils from patients with myelodysplasia. J Leukoc Biol *76*, 254-262.
Fuhler, G.M., Knol, G.J., Drayer, A.L., and Vellenga, E. (2005). Impaired interleukin-8- and GROalpha-induced phosphorylation of extracellular signal-regulated kinase result in decreased migration of neutrophils from patients with myelodysplasia. J Leukoc Biol *77*, 257-266.
Green, M.C., and Shultz, L.D. (1975). Motheaten, an immunodeficient mutant of the mouse. J Hered *66*, 250-258.
Gutierrez, N., Ocio, E., Rivas, J., Maiso, P., Delgado, M., Ferminan, E., Arcos, M., Sanchez, M., Hernandez, J., and San Miguel, J. (2007). Gene expression profiling of B lymphocytes and plasma cells from Waldenstrom's macroglobulinemia: composition with expression patterns of the same cell counterparts from chronic lymphocytic leukemia, multiple myeloma, and normal individuals. Leukemia *21*, 9.
Hahn, C.K., Berchuck, J.E., Ross, K.N., Kakoza, R.M., Clauser, K., Schinzel, A.C., Ross, L., Galinsky, I., Davis, T.N., Silver, S.J.*, et al.* (2009). Proteomic and genetic approaches identify Syk as an AML target. Cancer Cell *16*, 281-294.
Hamerman, J.A., Tchao, N.K., Lowell, C.A., and Lanier, L.L. (2005). Enhanced Toll-like receptor responses in the absence of signaling adaptor DAP12. Nat Immunol *6*, 579-586.

Hantschel, O., Warsch, W., Eckelhart, E., Kaupe, I., Grebien, F., Wagner, K.U., Superti-Furga, G., and Sexl, V. (2012). BCR-ABL uncouples canonical JAK2-STAT5 signaling in chronic myeloid leukemia. Nat Chem Biol *8*, 285-293.
Hibbs, M.L., Harder, K.W., Armes, J., Kountouri, N., Quilici, C., Casagranda, F., Dunn, A.R., and Tarlinton, D.M. (2002). Sustained activation of Lyn tyrosine kinase *in vivo* leads to autoimmunity. J Exp Med *196*, 12.
Holroyd, A., Cross, N.C., and Macdonald, D.H. (2011). The two faces of myeloproliferative neoplasms: Molecular events underlying lymphoid transformation. Leuk Res *35*, 1279-1285.
Hubbard, S.R. (2004). Juxtamembrane autoinhibition in receptor tyrosine kinases. Nat Rev Mol Cell Biol *5*, 464-471.
Hubbard, S.R., and Till, J.H. (2000). Protein tyrosine kinase structure and function. Annu Rev Biochem *69*, 373-398.
Iwasaki, H., and Akashi, K. (2007). Myeloid lineage commitment from the hematopoietic stem cell. Immunity *26*, 726-740.
Johnson, L.N., Noble, M.E., and Owen, D.J. (1996). Active and inactive protein kinases: structural basis for regulation. Cell *85*, 149-158.
Kales, S.C., Ryan, P.E., Nau, M.M., and Lipkowitz, S. (2010). Cbl and human myeloid neoplasms: the Cbl oncogene comes of age. Cancer Res *70*, 4789-4794.
Kanie, T., Abe, A., Matsuda, T., Kuno, Y., Towatari, M., Yamamoto, T., Saito, H., Emi, N., and Naoe, T. (2004). TEL-Syk fusion constitutively activates PI3-K/Akt, MAPK and JAK2-independent STAT5 signal pathways. Leukemia *18*, 548-555.
Kant, A.M., De, P., Peng, X., Yi, T., Rawlings, D.J., Kim, J.S., and Durden, D.L. (2002). SHP-1 regulates Fcgamma receptor-mediated phagocytosis and the activation of RAC. Blood *100*, 1852-1859.
Klampfl, T, A.H., Berg, T., Gisslinger, B., Schalling, M., Bagienski, K., Olcaydu, D., Passamonti, F., Rumi, E., Pietra, D., Jager, R., Pieri, L., Guglielmelli, P., Iacobucci, I., Martinelli, G., Cazzola, M., Vannucchi, A.M., Gisslinger, H. and Kralovics, R. (2011). Genome integrity of myeloproliferative neoplasms in chronic phase and during disease progression. Blood *118*, 167-176.
Kulathu, Y., Grothe, G., and Reth, M. (2009). Autoinhibition and adapter function of Syk. Immunol Rev *232*, 286-299.
Kulathu, Y., Hobeika, E., Turchinovich, G., and Reth, M. (2008). The kinase Syk as an adaptor controlling sustained calcium signalling and B-cell development. EMBO J *27*, 1333-1344.
Kuno, Y., Abe, A., Emi, N., Iida, M., Yokozawa, T., Towatari, M., Tanimoto, M., and Saito, H. (2001). Constitutive kinase activation of the TEL-Syk fusion gene in myelodysplastic syndrome with t(9;12)(q22;p12). Blood *97*, 1050-1055.
Layton, T., Stalens, C., Gunderson, F., Goodison, S., and Silletti, S. (2009). Syk tyrosine kinase acts as a pancreatic adenocarcinoma tumor suppressor by regulating cellular growth and invasion. Am J Pathol *175*, 2625-2636.
Lemmon, M.A., and Schlessinger, J. (2010). Cell signaling by receptor tyrosine kinases. Cell *141*, 1117-1134.
Levesque, J.P., and Winkler, I.G. (2011). Hierarchy of immature hematopoietic cells related to blood flow and niche. Curr Opin Hematol *18*, 220-225.

Lotem, J., and Sachs, L. (2002). Cytokine control of developmental programs in normal hematopoiesis and leukemia. Oncogene *21*, 3284-3294.
Meester-Smoor, M.A., Janssen, M.J., ter Haar, W.M., van Wely, K.H., Aarnoudse, A.J., van Oord, G., van Tilburg, G.B., and Zwarthoff, E.C. (2011). The ETS family member TEL binds to nuclear receptors RAR and RXR and represses gene activation. PloS one *6*, e23620.
Metcalf, D. (2007). On hematopoietic stem cell fate. Immunity *26*, 669-673.
Miller, A.L., Zhang, C., Shokat, K.M., and Lowell, C.A. (2009). Generation of a novel system for studying spleen tyrosine kinase function in macrophages and B cells. J Immunol *182*, 988-998.
Mocsai, A., Abram, C.L., Jakus, Z., Hu, Y., Lanier, L.L., and Lowell, C.A. (2006). Integrin signaling in neutrophils and macrophages uses adaptors containing immunoreceptor tyrosine-based activation motifs. Nat Immunol *7*, 1326-1333.
Mocsai, A., Humphrey, M.B., Van Ziffle, J., Hu, Y., Burghardt, A., Spusta, S.C., Majumdar, S., Lanier, L.L., Lowell, C.A., and Nakamura, M.C. (2004). The immunomodulatory adapter proteins DAP12 and Fc receptor γ-chain (FcRγ) regulate development of functional osteoclasts through the Syk tyrosine kinase. Proc Natl Acad Sci *101*, 6.
Mocsai, A., Ruland, J., and Tybulewicz, V.L. (2010). The SYK tyrosine kinase: a crucial player in diverse biological functions. Nat Rev Immunol *10*, 387-402.
Mocsai, A., Zhou, M., Meng, F., Tybulewicz, V.L., and Lowell, C.A. (2002). Syk is required for integrin signaling in neutrophils. Immunity *16*, 12.
Monti, S., Savage, K.J., Kutok, J.L., Feuerhake, F., Kurtin, P., Mihm, M., Wu, B., Pasqualucci, L., Neuberg, D., Agular, R.C.T.*, et al.* (2005). Molecular profiling of diffuse large B-cell lymphoma identifies robust subtypes including one characterized by host inflammatory response. Blood *105*, 1851-1861.
Moon, K.D., Post, C.B., Durden, D.L., Zhou, Q., De, P., Harrison, M.L., and Geahlen, R.L. (2005). Molecular basis for a direct interaction between the Syk protein-tyrosine kinase and phosphoinositide 3-kinase. J Biol Chem *280*, 1543-1551.
Moroni, M., Soldatenkov, V., Zhang, L., Zhang, Y., Stoica, G., Gehan, E., Rashidi, B., Singh, B., Ozdemirli, M., and Mueller, S.C. (2004). Progressive loss of Syk and abnormal proliferation in breast cancer cells. Cancer Res *64*, 7346-7354.
Murray, P.J. (2007). The JAK-STAT signaling pathway: input and output integration. J Immunol *178*, 2623-2629.
Muthusamy, V., Duraisamy, S., Bradbury, C.M., Hobbs, C., Curley, D.P., Nelson, B., and Bosenberg, M. (2006). Epigenetic silencing of novel tumor suppressors in malignant melanoma. Cancer Res *66*, 11187-11193.
Nathan, C. (2006). Neutrophils and immunity: challenges and opportunities. Nat Rev Immunol *6*, 173-182.
Ogawa, M. (1993). Differentiation and proliferation of hematopoietic stem cells. Blood *81*, 2844-2853.
Okazawa, H., Motegi, S., Ohyama, N., Ohnishi, H., Tomizawa, T., Kaneko, Y., Oldenborg, P.A., Ishikawa, O., and Matozaki, T. (2005). Negative regulation of phagocytosis in macrophages by the CD47-SHPS-1 system. J Immunol *174*, 2004-2011.
Palacios, E.H., and Weiss, A. (2007). Distinct roles for Syk and ZAP-70 during early thymocyte development. J Exp Med *204*, 1703-1715.

Paolini, R., Molfetta, R., Beitz, L.O., Zhang, J., Scharenberg, A.M., Piccoli, M., Frati, L., Siraganian, R., and Santoni, A. (2002). Activation of Syk tyrosine kinase is required for c-Cbl-mediated ubiquitination of Fcepsilon RI and Syk in RBL cells. J Biol Chem *277*, 36940-36947.
Pardanani, A., Finke, C., Lasho, T.L., Al-Kali, A., Begna, K.H., Hanson, C.A., and Tefferi, A. (2012). IPSS-independent prognostic value of plasma CXCL10, IL-7 and IL-6 levels in myelodysplastic syndromes. Leukemia *26*, 693-699.
Passegue, E., Jamieson, C.H., Ailles, L.E., and Weissman, I.L. (2003). Normal and leukemic hematopoiesis: are leukemias a stem cell disorder or a reacquisition of stem cell characteristics? Proc Natl Acad Sci U S A *100 Suppl 1*, 11842-11849.
Pieri, L., Bogani, C., Guglielmelli, P., Zingariello, M., Rana, R.A., Bartalucci, N., Bosi, A., and Vannucchi, A.M. (2009). The JAK2V617 mutation induces constitutive activation and agonist hypersensitivity in basophils from patients with polycythemia vera. Haematologica *94*, 1537-1545.
Quintas-Cardama, A., Kantarjian, H., Cortes, J., and Verstovsek, S. (2011). Janus kinase inhibitors for the treatment of myeloproliferative neoplasias and beyond. Nat Rev Drug Disc *10*, 127-140.
Raaijmakers, M.H., Mukherjee, S., Guo, S., Zhang, S., Kobayashi, T., Schoonmaker, J.A., Ebert, B.L., Al-Shahrour, F., Hasserjian, R.P., Scadden, E.O.*, et al.* (2010). Bone progenitor dysfunction induces myelodysplasia and secondary leukaemia. Nature *464*, 852-857.
Reynaud, D., Pietras, E., Barry-Holson, K., Mir, A., Binnewies, M., Jeanne, M., Sala-Torra, O., Radich, J.P., and Passegue, E. (2011). IL-6 controls leukemic multipotent progenitor cell fate and contributes to chronic myelogenous leukemia development. Cancer Cell *20*, 661-673.
Rigby, S., Huang, Y., Streubel, B., Chott, A., Du, M.Q., Turner, S.D., and Bacon, C.M. (2009). The lymphoma-associated fusion tyrosine kinase ITK-SYK requires pleckstrin homology domain-mediated membrane localization for activation and cellular transformation. J Biol Chem *284*, 26871-26881.
Rinaldi, A., Kwee, I., Taborelli, M., Largo, C., Uccella, S., Martin, V., Poretti, G., Gaidano, G., Calabrese, G., Martinelli, G.*, et al.* (2005). Genomic and expression profiling identifies the B-cell associated tyrosine kinase Syk as a possible therapeutic target in mantle cell lymphoma. Brit J Haematol *132*, 14.
Ross, E.A., Anderson, N., and Micklem, H.S. (1982). Serial depletion and regeneration of the murine hematopoietic system. Implications for hematopoietic organization and the study of cellular aging. J Exp Med *155*, 432-444.
Rothenberg, E.V. (2007). Negotiation of the T lineage fate decision by transcription-factor interplay and microenvironmental signals. Immunity *26*, 690-702.
Rowley, J.D. (1973). Letter: A new consistent chromosomal abnormality in chronic myelogenous leukaemia identified by quinacrine fluorescence and Giemsa staining. Nature *243*, 290-293.
Sada, K., Takano, T., Yanagi, S., and Yamamura, H. (2001). Structure and function of Syk protein-tyrosine kinase. J Biochemistry *130*, 10.
Simon, M., Vanes, L., Geahlen, R.L., and Tybulewicz, V.L. (2005). Distinct roles for the linker region tyrosines of Syk in FcepsilonRI signaling in primary mast cells. J Biol Chem *280*, 4510-4517.

Soboloff, J., Rothberg, B.S., Madesh, M., and Gill, D.L. (2012). STIM proteins: dynamic calcium signal transducers. Nat Rev Mol Cell Biol *13*, 549-565.
Streubel, B., Vinatzer, U., Willheim, M., Raderer, M., and Chott, A. (2006). Novel t(5;9)(q33;q22) fuses ITK to SYK in unspecified peripheral T-cell lymphoma. Leukemia *20*, 313-318.
Sun, L., Hwang, W.Y., and Aw, S.E. (2006). Biological characteristics of megakaryocytes: specific lineage commitment and associated disorders. Int J Biochem Cell Biol *38*, 1821-1826.
Sung, Y.M., Xu, X., Sun, J., Mueller, D., Sentissi, K., Johnson, P., Urbach, E., Seillier-Moiseiwitsch, F., Johnson, M.D., and Mueller, S.C. (2009). Tumor suppressor function of Syk in human MCF10A in vitro and normal mouse mammary epithelium in vivo. PLoS One *4*, e7445.
Takeda, Y., Nakaseko, C., Tanaka, H., Takeuchi, M., Yui, M., Saraya, A., Miyagi, S., Wang, C., Tanaka, S., Ohwada, C.*, et al.* (2011). Direct activation of STAT5 by ETV6-LYN fusion protein promotes induction of myeloproliferative neoplasm with myelofibrosis. Brit J Haematol *153*, 589-598.
Tanaka, H., Takeuchi, M., Takeda, Y., Sakai, S., Abe, D., Ohwada, C., Sakaida, E., Shimizu, N., Saito, Y., Miyagi, S.*, et al.* (2010). Identification of a novel TEL-Lyn fusion gene in primary myelofibrosis. Leukemia *24*, 197-200.
Tefferi, A. (2008). The history of myeloproliferative disorders: before and after Dameshek. Leukemia *22*, 3-13.
Tefferi, A. (2010). Novel mutations and their functional and clinical relevance in myeloproliferative neoplasms: JAK2, MPL, TET2, ASXL1, CBL, IDH and IKZF1. Leukemia *24*, 1128-1138.
Tefferi, A. (2012). Myeloproliferative neoplasms 2012: The John M. Bennett 80th birthday anniversary lecture. Leuk Res *36*, 1481-1489.
Tefferi, A., Vaidya, R., Caramazza, D., Finke, C., Lasho, T., and Pardanani, A. (2011). Circulating interleukin (IL)-8, IL-2R, IL-12, and IL-15 levels are independently prognostic in primary myelofibrosis: a comprehensive cytokine profiling study. J Clin Onco *29*, 1356-1363.
Thiele, J., and Kvasnicka, H.M. (2005). Hematopathologic findings in chronic idiopathic myelofibrosis. Sem Onco *32*, 380-394.
Thomas, D.H., Getz, T.M., Newman, T.N., Dangelmaier, C.A., Carpino, N., Kunapuli, S.P., Tsygankov, A.Y., and Daniel, J.L. (2010). A novel histidine tyrosine phosphatase, TULA-2, associates with Syk and negatively regulates GPVI signaling in platelets. Blood *116*, 2570-2578.
Till, J.E., and McCulloch, E.A. (1961). A direct measurement of the radiation sensitivity of normal mouse bone marrow cells. Radiat Res *14*, 213-222.
Toyama, T., Iwase, H., Yamashita, H., Hara, Y., Omoto, Y., Sugiura, H., Zhang, Z., and Fujii, Y. (2003). Reduced expression of the Syk gene is correlated with poor prognosis in human breast cancer. Cancer Lett *189*, 97-102.
Turner, M.P., Mee, J., Costello, P.S., Williams, O., Price, A.A., Duddy, L.P., Furlong, M.T., Geahlen, R.L., and Tybulewicz, V.L. (1995). Perinatal lethality and blocked B-cell development in mice lacking the tyrosine kinase Syk. Nature *378*, 298-302.

Vaidya, R., Gangat, N., Jimma, T., Finke, C.M., Lasho, T.L., Pardanani, A., and Tefferi, A. (2012). Plasma cytokines in polycythemia vera: Phenotypic correlates, prognostic relevance, and comparison with myelofibrosis. Am J Hematol *87*, 1003-1005.
Vainchenker, W., Delhommeau, F., Constantinescu, S.N., and Bernard, O.A. (2011). New mutations and pathogenesis of myeloproliferative neoplasms. Blood *118*, 1723-1735.
Van Etten, R.A. (2002). Studying the pathogenesis of BCR-ABL+ leukemia in mice. Oncogene *21*, 8643-8651.
Vardiman, J.W., Thiele, J., Arber, D.A., Brunning, R.D., Borowitz, M.J., Porwit, A., Harris, N.L., Le Beau, M.M., Hellstrom-Lindberg, E., Tefferi, A.*, et al.* (2009). The 2008 revision of the World Health Organization (WHO) classification of myeloid neoplasms and acute leukemia: rationale and important changes. Blood *114*, 937-951.
Wang, D., Feng, J., Wen, R., Marine, J.C., Sangster, M.Y., Parganas, E., Hoffmeyer, A., Jackson, C.W., Cleveland, J.L., Murray, P.J.*, et al.* (2000). Phospholipase Cgamma2 is essential in the functions of B cell and several Fc receptors. Immunity *13*, 25-35.
Weissman, I.L., Anderson, D.J., and Gage, F. (2001). Stem and progenitor cells: origins, phenotypes, lineage commitments, and transdifferentiations. Annu Rev Cell Dev Biol *17*, 387-403.
Wen, R., Jou, S.T., Chen, Y., Hoffmeyer, A., and Wang, D. (2002). Phospholipase C gamma 2 is essential for specific functions of Fc epsilon R and Fc gamma R. J Immunol *169*, 6743-6752.
Wossning, T., Herzog, S., Kohler, F., Meixlsperger, S., Kulathu, Y., Mittler, G., Abe, A., Fuchs, U., Borkhardt, A., and Jumaa, H. (2006). Deregulated Syk inhibits differentiation and induces growth factor-independent proliferation of pre-B cells. J Exp Med *203*, 2829-2840.
Wu, L., and Liu, Y.J. (2007). Development of dendritic-cell lineages. Immunity *26*, 741-750.
Yuan, H., Wang, Z., Li, L., Zhang, H., Modi, H., Horne, D., Bhatia, R., and Chen, W. (2012). Activation of stress response gene SIRT1 by BCR-ABL promotes leukemogenesis. Blood, *119*, 1904-1914.
Zhang, H., Li, H., Xi, H.S., and Li, S. (2012). HIF1alpha is required for survival maintenance of chronic myeloid leukemia stem cells. Blood *119*, 2595-2607.
Zhang, J., Berenstein, E., and Siraganian, R.P. (2002). Phosphorylation of Tyr342 in the linker region of Syk is critical for FcεRI signaling in mast cells. Mol Cell Biol *22*, 11.
Zhang, J., Billingsley, M.L., Kincaid, R.L., and Siraganian, R.P. (2000). Phosphorylation of Syk activation loop tyrosines is essential for Syk function. An in vivo study using a specific anti-Syk activation loop phosphotyrosine antibody. J Biol Chem *275*, 35442-35447.
Zhang, J., Kimura, T., and Siraganian, R.P. (1998). Mutations in the activation loop tyrosines of protein tyrosine kinase Syk abrogate intracellular signaling but not kinase activity. J Immunol *161*, 4366-4374.
Zhang, Y., Oh, H., Burton, R.A., Burgner, J.W., Gaehlen, R.L., and Post, C.B. (2008). Tyr130 phosphorylation triggers Syk release from antigen receptor by long-distance conformational uncoupling. Proc Natl Acad Sci *105*, 11760-11765.

Zou, W., Reeve, J.L., Zhao, H., Ross, F.P., and Teitelbaum, S.L. (2009). Syk tyrosine 317 negatively regulates osteoclast function via the ubiquitin-protein isopeptide ligase activity of Cbl. J Biol Chem *284*, 18833-18839.

Publishing Agreement

It is the policy of the University to encourage the distribution of all theses, dissertations, and manuscripts. Copies of all UCSF theses, dissertations, and manuscripts will be routed to the library via the Graduate Division. The library will make all theses, dissertations, and manuscripts accessible to the public and will preserve these to the best of their abilities, inperpetuity.

I hereby grant permission to the Graduate Division of the University of California, San Francisco to release copies of my thesis, dissertation, or manuscript to the Campus Library to provide access and preservation, in whole or in part, in perpetuity.

Michelle J. Graham — Author Signature

12/20/12 — Date